Searches for Lepton Flavor Violation

An Experimental Review

David Hitlin
Caltech
DISCRETE 2021
December 2, 2021

Charged lepton flavor violation (CLFV)

- CLFV denotes a transition involving μ, e and τ lepton states that doesn't conserve lepton family number, *i.e.*, there are no neutrinos involved
  - A CLF conserving transition: $\mu^- \to e^- \nu_e \bar{\nu}_\mu$
  - A CLFV transition: $\mu \to e\gamma$, $\mu \to 3e$, $\mu N \to e N$ ($\mu \to e$ conversion)
- Family number is not a symmetry of the Standard Model Lagrangian
  - Quark family number is violated in weak decays (*c.f.* the CKM matrix)
  - Neutrino oscillations are proof of the violation of neutral lepton flavor conservation as well as evidence for BSM physics (*e.g.,* see-saw)
- A natural question: "Is there also observable charged lepton flavor violation?"
  - In the Standard Model (+ heavy neutrinos), CLFV is very small:

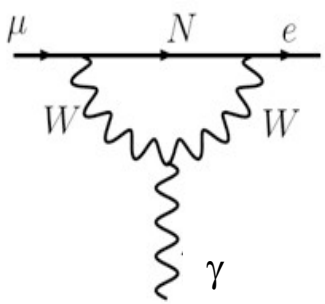

$$\mathcal{B}(\mu \to e\gamma) = \frac{3\alpha}{32\pi} \left| \sum_{i=2,3} U^*_{\mu i} U_{ei} \frac{\Delta m^2_{1i}}{M^2_W} \right|^2 < 10^{-54}$$

  - Thus CLFV searches are a clean probe of NP in the charged lepton sector

Searching for CLFV

- Many NP models predict CLFV processes to occur in an observable regime
- The sensitivity to CLFV in loop processes can exceed that in direct production
  - There are many distinct experimental probes and a rich phenomenology, leading to a robust experimental scene
    - $\mu \to e\gamma$: most powerful limits: MEG-II at PSI
    - $\mu N \to e N$ muon to electron conversion: three experiments upcoming: Mu2e at FNAL and DeeMe and COMET at JPARC

$$R_{\mu e} = \frac{\Gamma(\mu^- + N(A,Z) \to e^- + N(A,Z))}{\Gamma(\mu^- + N(A,Z) \to \text{all muon captures})}$$

    - $\mu \to 3e$: Mu3e at PSI
    - $\mu^- N \to e^+ N(Z\text{-}2)$ (Mu2e–II, COMET Phase 2?)
    - $\mu^+ e^- \to \mu^- e^+$
    - $\tau \to (e,\mu)\gamma$ and many other τ decays (Belle II)
    - $H^0 \to \mu, e, \tau + X$ (LHC)
    - $K_L \to \mu e$, $B \to \mu e$, $K \to \mu e$, ... (LHCb, expts at J-PARC, CERN)
  - The form of the CLFV Yukawa coupling matrix is model-dependent, *e.g.*, it could be PMNS-like or CKM-like
  - Different theories predict distinct correlations between CLFV processes

CLFV Processes

- Low energy probes: rare μ, τ and H^0 decays, $\mu \to e$ conversion, CLFV in meson decay

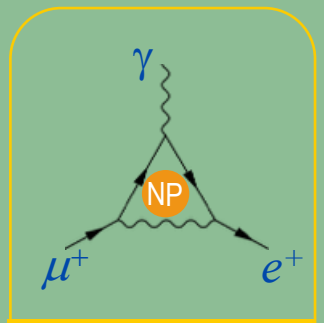

$\mu^+ \to e^+\gamma$

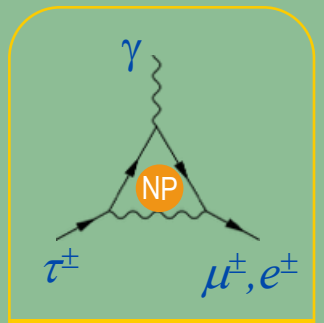

$\tau \to \mu\gamma$, eγ

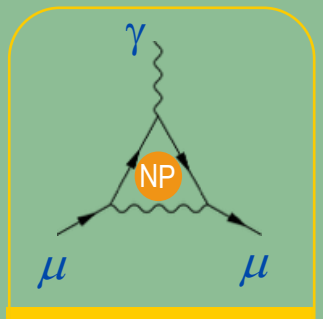

$(g\text{-}2)_\mu$

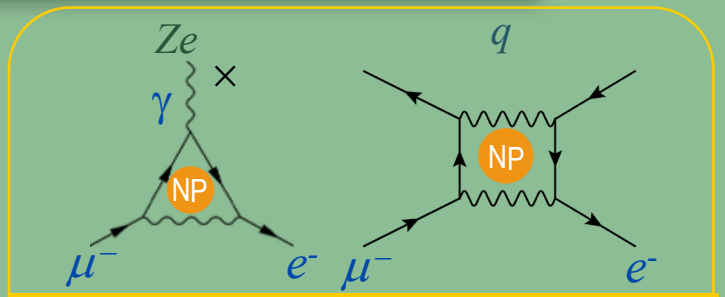

$\mu^- N \to e^- N$

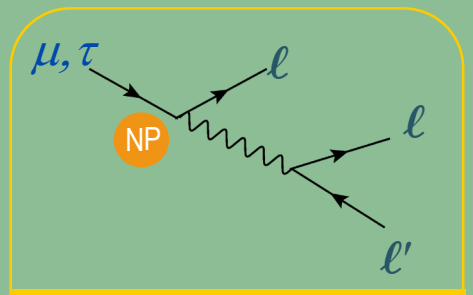

$\mu, \tau \to 3\ell$

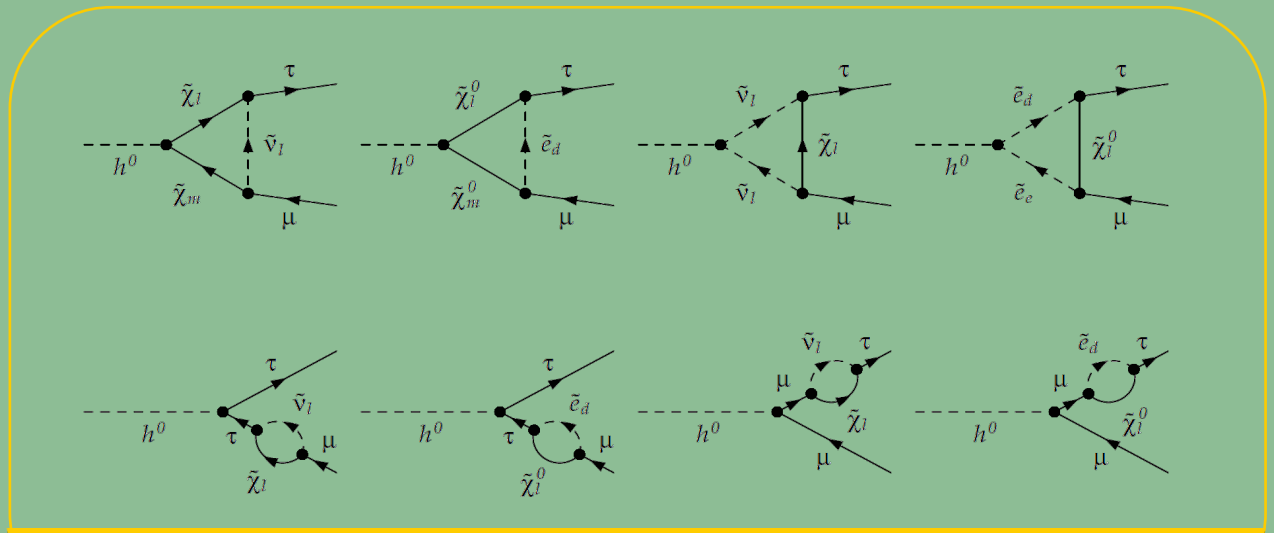

Higgs decay: $H^0 \to \tau\,\mu$ (also $\tau\, e$, $\mu\, e$)

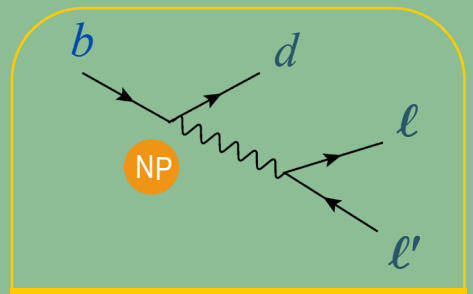

$B \to \ell\ell'$

$B \to X_s \ell\ell'$

New Physics contributions to $\mu \to e$ conversion

$\mu N \to eN$ is sensitive to a wide variety of New Physics models, *e.g.*, SUSY, 2HDM, Extra Dimensions, Leptoquarks, GUTs, LHT,…

Supersymmetry

rate ~ 10^{-15}

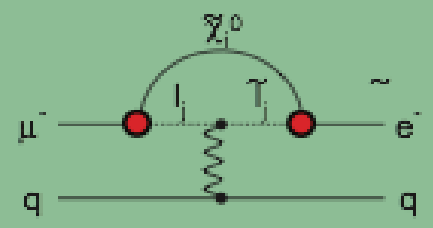

Compositeness

Λ_c ~ 3000 TeV

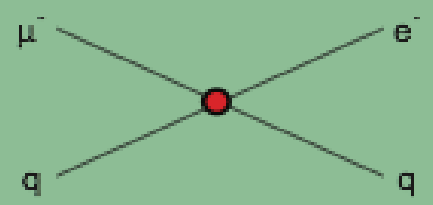

Leptoquark

M_{LQ} = 3000 $(\lambda_{\mu d}\lambda_{ed})^{1/2}$ TeV/c^2

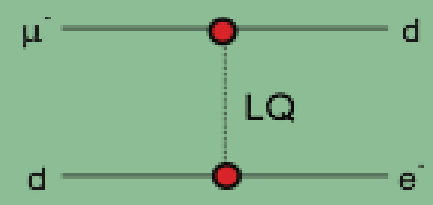

Heavy Neutrinos

$|U_{\mu N}U_{eN}|^2$ ~ 8×10^{-13}

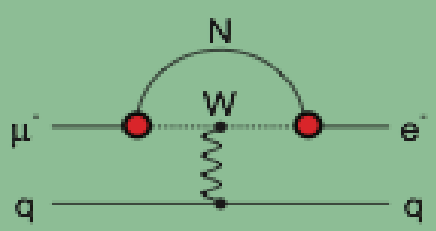

Second Higgs Doublet

$g(H_{\mu e})$ ~ $10^{-4} g(H_{\mu\mu})$

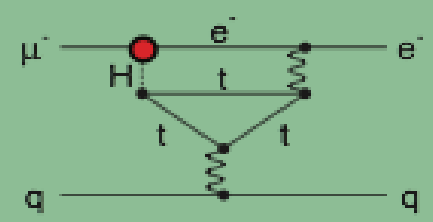

Heavy *Z'* Anomalous *Z* Coupling

$M_{Z'}$ = 3000 TeV/c^2

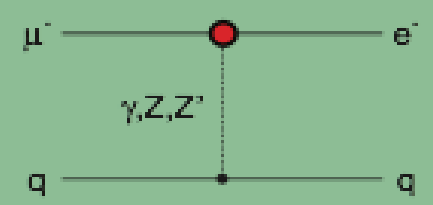

Model-independent effective Lagrangian

$$\mathcal{L}_{\mathrm{CLFV}} = \frac{m_\mu}{(1+\kappa)\Lambda^2}\bar{\mu}_R \sigma_{\mu\nu} e_L F^{\mu\nu} \quad + \quad \frac{\kappa}{(1+\kappa)\Lambda^2}\bar{\mu}_L \gamma_\mu e_L (\bar{u}_L \gamma_\mu u_L + \bar{d}_L \gamma_\mu d_L) \quad + h.c.$$

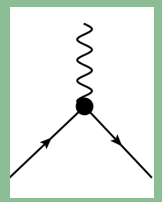

Dipole interaction
(SUSY, ……)

$\mu \to e\gamma$

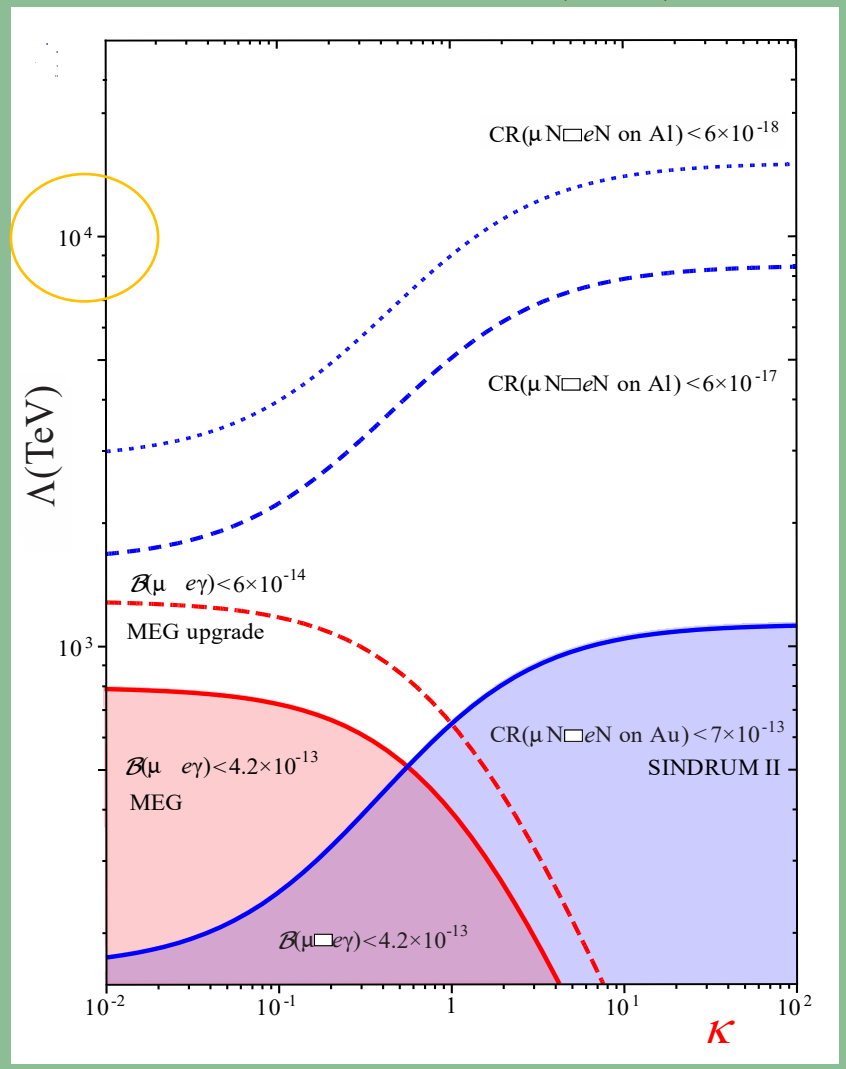

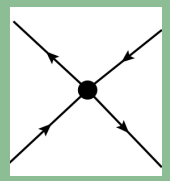

Contact interaction
(Z', leptoquarks, …

$\mu \to e$ conversion

CLFV processes have unique sensitivity to New Physics at high mass scales

Also $\mu \to eee$

Derived from A. de Gouvêa & P. Vogel, Prog.Part.Nucl. Phys 71, 75 (2013)

Purely leptonic case: $\mu \to e\gamma$, $\mu \to 3e$ $(\tau \to)$

$$\mathcal{L}_{\mathrm{CLFV}} = \frac{m_\mu}{(1+\kappa)\Lambda^2}\bar{\mu}_R \sigma_{\mu\nu} e_L F^{\mu\nu} + \frac{\kappa}{(1+\kappa)\Lambda^2}\bar{\mu}_L \gamma_\mu e_L (\bar{e}_L \gamma_\mu e_L) + h.c.$$

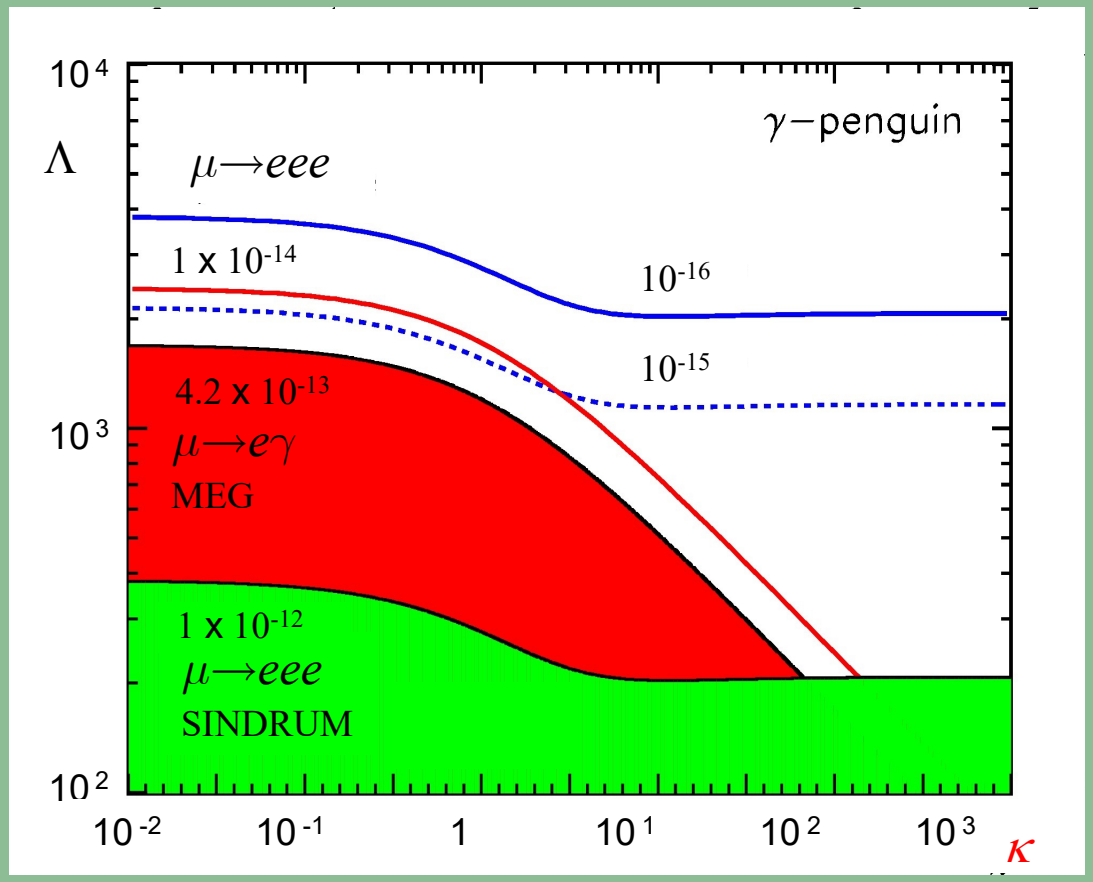

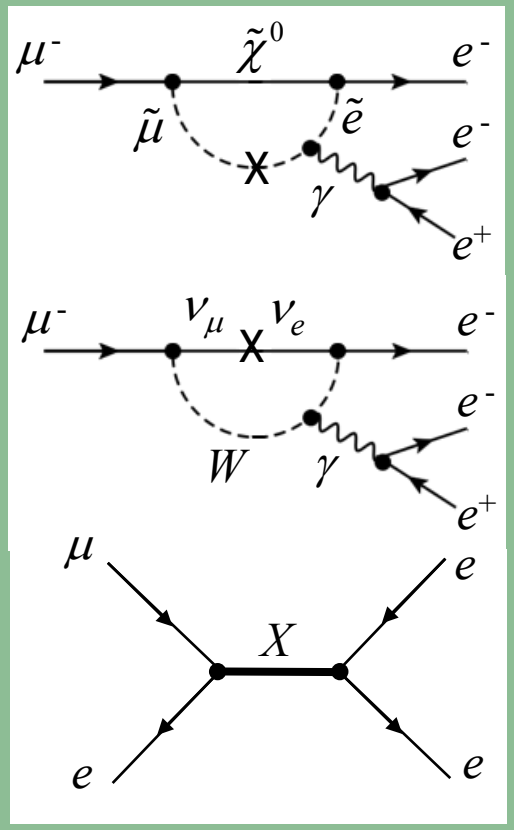

Hisano

Effective Field Theory treatment

- $\mu \to e$ expts probe multi-loop effects in NP theories with a greater Λ_{NP} reach than LHC
- CLFV BSM contact interactions can be parametrized by a set of 2, 3 and 4 point functions that respect QED and QCD:

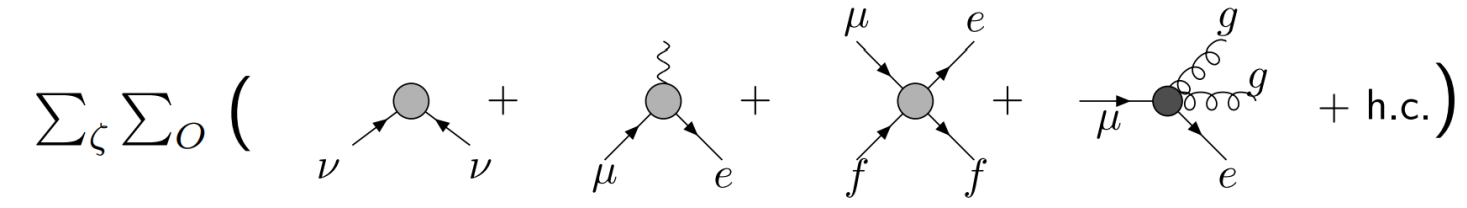

- These can be evaluated as loops in EFT in a model-independent manner
  - Loops rescale the couplings and can mix interactions
- For $\mu \to e\gamma$, $\mu \to 3e$, $\mu N \to e N$ there are a total of 82 operators
- A combination of limits or observations of the three processes can help to isolate those operators involved in particular models
- In particular, the Z dependence of $\mu N \to e N$ can be an important tool
  - In $\mu \to e$ conversion, different nuclei with different spins pick out particular linear combinations of new physics operators

Crivellin, Davidson, Pruna, Signer, JHEP 05, 117, 2017
Cirigliano, Davidson, Kuno, Phys.Lett. B 771, 242, 2017
Davidson, Kuno,Yamanaka, Phys.Lett. B 790, 380, 2019
Davidson, *JHEP* 02, 172, 2021

Current and future CLFV limits (90%CL)

Process	Current Limit	Next Generation exp
$\tau \to \mu\eta$	BR < 6.5 x 10^{-8}	
$\tau \to \mu\gamma$	BR < 6.8 x 10^{-8}	10^{-9} - 10^{-10} (Belle II)
$\tau \to \mu\mu\mu$	BR < 3.2 x 10^{-8}	
$\tau \to eee$	BR < 3.6 x 10^{-8}	
$K_L \to e\mu$	BR < 4.7 x 10^{-12}	
$K^+ \to \pi^+ e^- \mu^+$	BR < 1.3 x 10^{-11}	
$B^0 \to e\mu$	BR < 7.8 x 10^{-8}	
$B^+ \to K^+ e\mu$	BR < 9.1 x 10^{-8}	
$\mu^+ \to e^+\gamma$	BR < 6.1 x x 10^{-13}	10^{-14} (MEG-II)
$\mu^+ \to e^+e^+e^-$	BR < 1.0 x 10^{-12}	10^{-16} (Mu3e)
$\mu N \to eN$	$R_{\mu e}$ < 7.0 x 10^{-13}	10^{-17} (Mu2e, COMET, DeeMe)

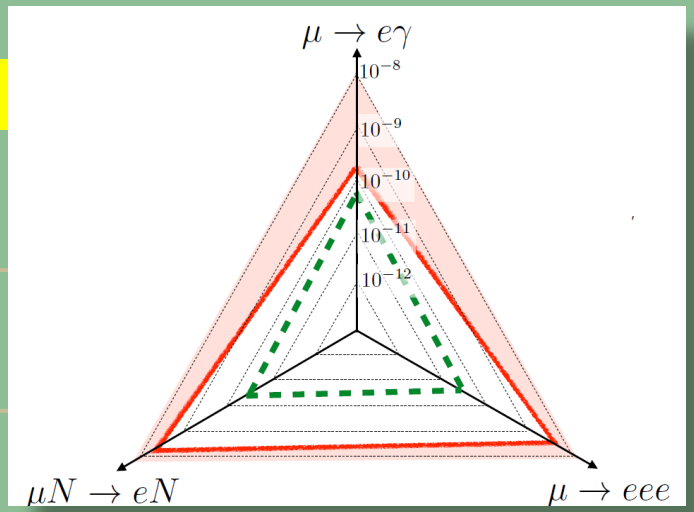

$C^{\mu e}_{e\gamma}$ from present limits

$C^{\mu e}_{e\gamma}$ from future experiments

Calibbi and Signorelli
arXiv: 1709.00294 [hep-ph]

Bounds on Higgs exchange models

- Bounds on CLFV couplings to the Higgs can be derived from LHC limits as well as conventional leptonic processes

$$\begin{pmatrix} Y_{ee} & Y_{e\mu} & Y_{e\tau} \\ Y_{\mu e} & Y_{\mu\mu} & Y_{\mu\tau} \\ Y_{\tau e} & Y_{e\mu} & Y_{\tau\tau} \end{pmatrix}$$

$$\mathcal{L}_Y \supset -Y_{e\mu}\bar{e}_L\mu_R h - Y_{\mu e}\bar{\mu}_L e_R h - Y_{e\tau}\bar{e}_L\tau_R h - Y_{\tau e}\bar{\tau}_L e_R h - Y_{\mu\tau}\bar{\mu}_L\tau_R h - Y_{\tau\mu}\bar{\tau}_L\mu_R h + h.c..$$

CLFV Higgs decay $\quad \Gamma(h \to \ell^\alpha \ell^\beta) = \frac{m_h}{8\pi}\left(|Y_{\ell^\beta \ell^\alpha}|^2 + |Y_{\ell^\alpha \ell^\beta}|^2\right)$

$\mu \to e\gamma \;\; (\tau \to \mu\gamma)$

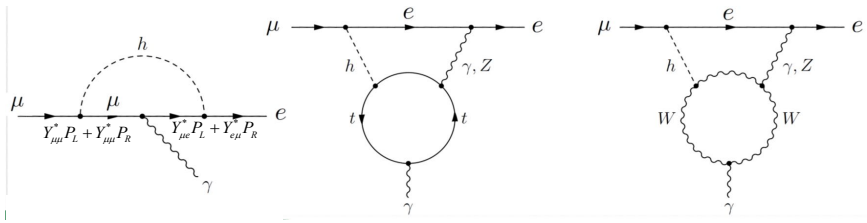

$\mu \to 3e \;\; (\tau \to \ell'\ell\ell)$

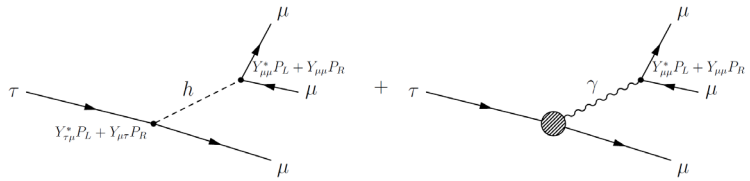

$\mu N \to eN$

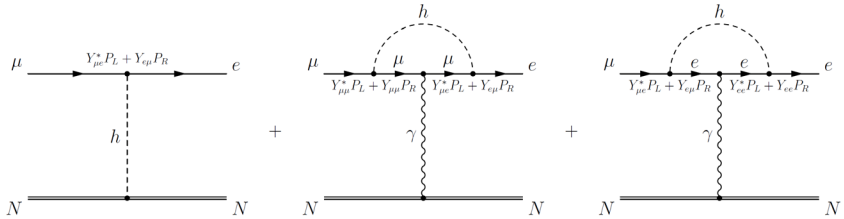

g-2

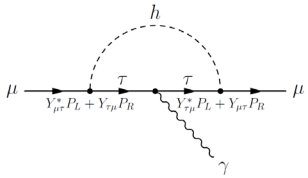

Higgs CLFV

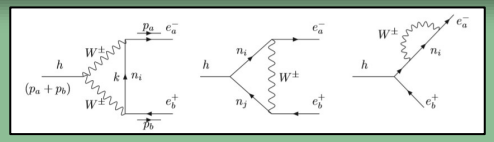

(R.Harnik, et al., JHEP 03 (2013) 026)
updated

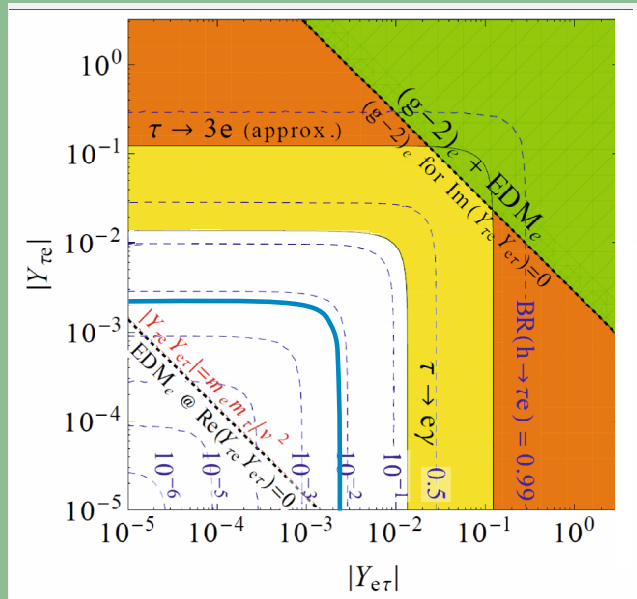

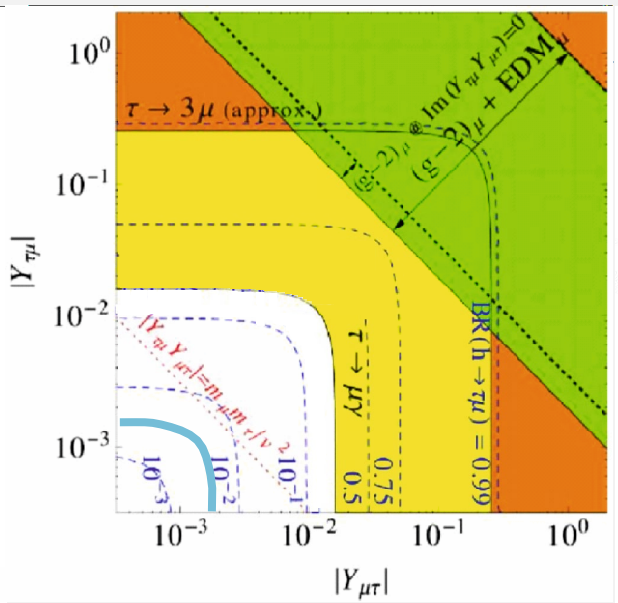

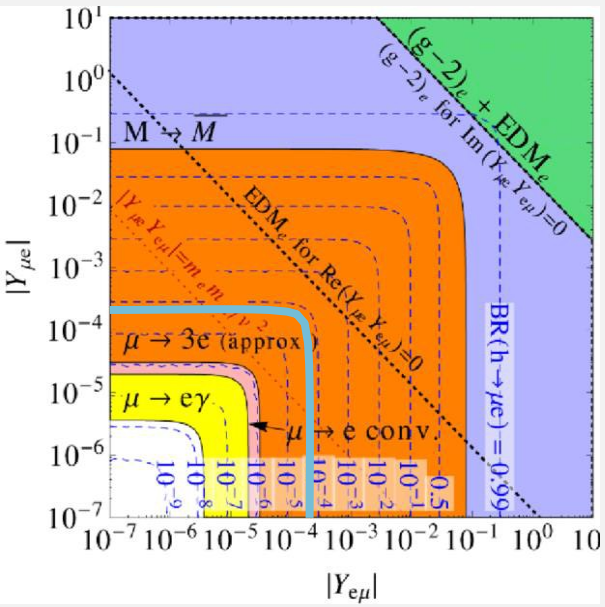

< 4.7×10^{-3} @ 95% CL ATLAS 2020 13 TeV, 36.1 fb^{-1}	< 2.5×10^{-3} @ 95% CL CMS 2018 13 TeV, 35.9 fb^{-1}	< 6.1×10^{-5} @ 95% CL ATLAS 2020 13 TeV, 39 fb^{-1}

- CLFV Higgs couplings to τ (τe, $\tau \mu$) can likely be best measured at the LHC
- μe couplings are best measured in dedicated muon experiments

Model discrimination through correlations

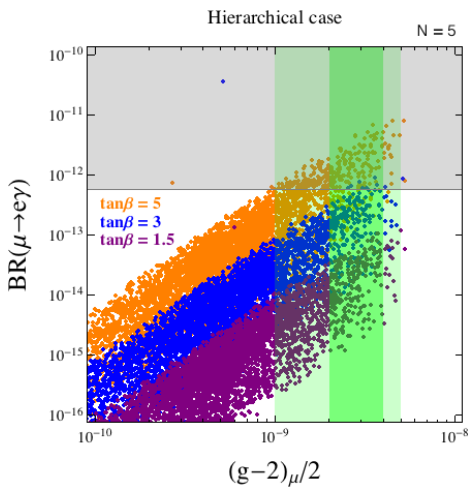

Calibbi *et al.*
arXiv:1408.0754 [hep-ph]

arXiv:0702136v3 [hep-ph]

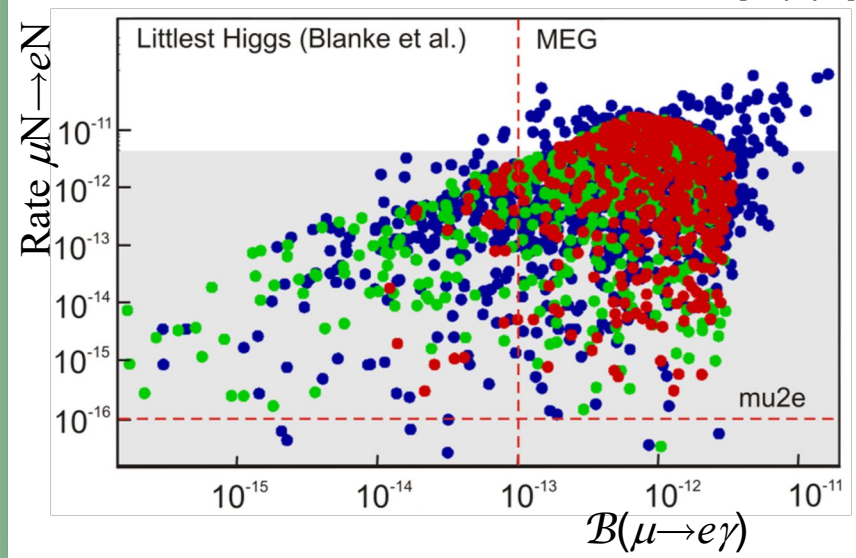

A. Vicente & C.E. Yaguna – Scotogenic model, N_1-N_1 annihilation region

arXiv: 1412.2545 [hep-ph]

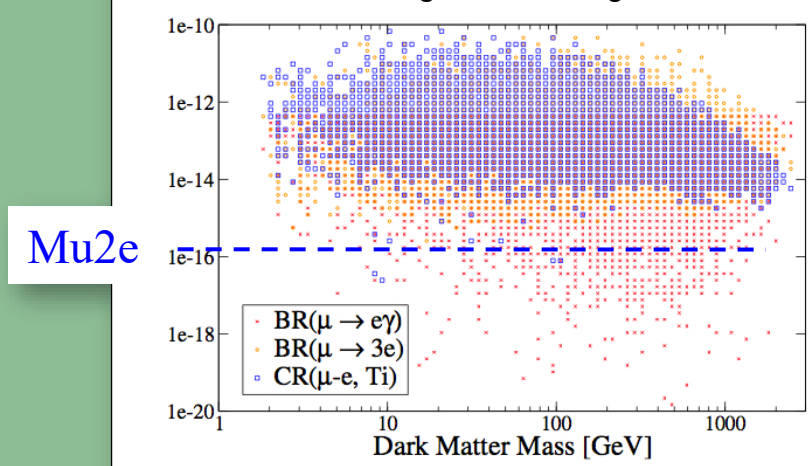

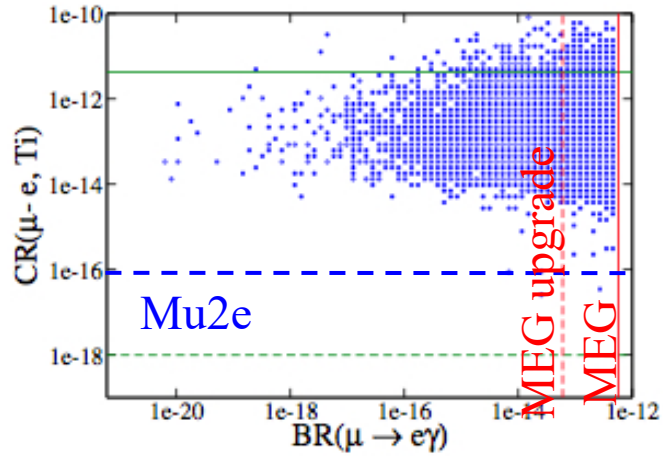

Model discrimination through correlations

ratio	LHT	MSSM (dipole)	MSSM (Higgs)
$\frac{Br(\mu^- \to e^- e^+ e^-)}{Br(\mu \to e\gamma)}$	$0.02\ldots1$	$\sim 6\cdot10^{-3}$	$\sim 6\cdot10^{-3}$
$\frac{Br(\tau^- \to e^- e^+ e^-)}{Br(\tau \to e\gamma)}$	$0.04\ldots0.4$	$\sim 1\cdot10^{-2}$	$\sim 1\cdot10^{-2}$
$\frac{Br(\tau^- \to \mu^- \mu^+ \mu^-)}{Br(\tau \to \mu\gamma)}$	$0.04\ldots0.4$	$\sim 2\cdot10^{-3}$	$0.06\ldots0.1$
$\frac{Br(\tau^- \to e^- \mu^+ \mu^-)}{Br(\tau \to e\gamma)}$	$0.04\ldots0.3$	$\sim 2\cdot10^{-3}$	$0.02\ldots0.04$
$\frac{Br(\tau^- \to \mu^- e^+ e^-)}{Br(\tau \to \mu\gamma)}$	$0.04\ldots0.3$	$\sim 1\cdot10^{-2}$	$\sim 1\cdot10^{-2}$
$\frac{Br(\tau^- \to e^- e^+ e^-)}{Br(\tau^- \to e^- \mu^+ \mu^-)}$	$0.8\ldots2.0$	~ 5	$0.3\ldots0.5$
$\frac{Br(\tau^- \to \mu^- \mu^+ \mu^-)}{Br(\tau^- \to \mu^- e^+ e^-)}$	$0.7\ldots1.6$	~ 0.2	$5\ldots10$
$\frac{R(\mu\mathrm{Ti} \to e\mathrm{Ti})}{Br(\mu \to e\gamma)}$	$10^{-3}\ldots10^{2}$	$\sim 5\cdot10^{-3}$	$0.08\ldots0.15$

Correlations in the $\tau \to \mu\gamma$ and $\ell\ell\ell$ branching fractions

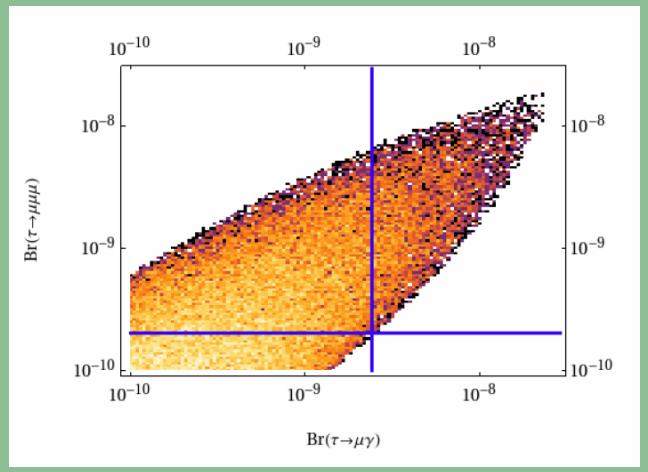

Blanke, Buras, Duling, Recksiegel & Tarantino, Acta Phys. Polon. B41, 657 (2010)

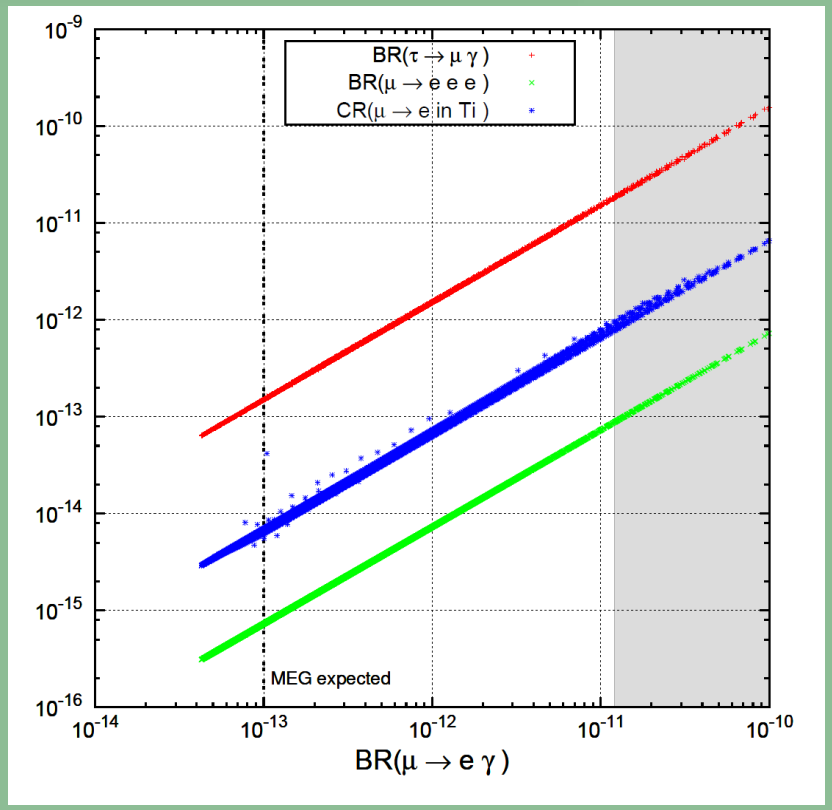

$\mathcal{B}(\tau \to \mu\gamma)$ *vs.* $\mathcal{B}(\mu \to eee)$ and $\mathrm{CR}(\mu \to \mathrm{e\ on\ Ti})$ in an SO(10) Type II SUSY model
Calibbi, et al., JHEP 0912 057 (2009)

CLFV Physics Reach

★★★ = Discovery Sensitivity

	AC	RVV2	AKM	δLL	FBMSSM	LHT	RS
$D^0 - \bar{D}^0$	★★★	★	★	★	★	★★★	?
ϵ_K	★	★★★	★★★	★	★	★★	★★★
$S_{\psi\phi}$	★★★	★★★	★★★	★	★	★★★	★★★
$S_{\phi K_S}$	★★★	★★	★	★★★	★★★	★	?
$A_{\rm CP}(B \to X_s\gamma)$	★	★	★	★★★	★★★	★	?
$A_{7,8}(B \to K^*\mu^+\mu^-)$	★	★	★	★★★	★★★	★★	?
$A_9(B \to K^*\mu^+\mu^-)$	★	★	★	★	★	★	?
$B \to K^{(*)}\nu\bar{\nu}$	★	★	★	★	★	★	★
$B_s \to \mu^+\mu^-$	★★★	★★★	★★★	★★★	★★★	★	★
$K^+ \to \pi^+\nu\bar{\nu}$	★	★	★	★	★	★★★	★★★
$K_L \to \pi^0\nu\bar{\nu}$	★	★	★	★	★	★★★	★★★
$\mu \to e\gamma$	★★★	★★★	★★★	★★★	★★★	★★★	★★★
$\tau \to \mu\gamma$	★★★	★★★	★	★★★	★★★	★★★	★★★
$\mu + N \to e + N$	★★★	★★★	★★★	★★★	★★★	★★★	★★★
d_n	★★★	★★★	★★★	★★	★★★	★	★★★
d_e	★★★	★★★	★★	★	★★★	★	★★★
$(g-2)_\mu$	★★★	★★★	★★	★★★	★★★	★	?

Table 8: "DNA" of flavour physics effects for the most interesting observables in a selection of SUSY and non-SUSY models ★★★ signals large effects, ★★ visible but small effects and ★ implies that the given model does not predict sizable effects in that observable.

W. Altmannshofer, A.J.Buras, S.Gori, P.Paradisi, D.M.Straub
Nucl.Phys.B 830, 17 (2010)

Glossary

AC	U(1) flavor symmetry
RVV2	Non-abelian
AKM	SU(3)
δLL	Left-handed CKM-like
FBMSSM	Flavor-blind MSSM
LHT	Littlest Higgs w T-Parity
RS	Randall-Sundrum

Excellent sensitivity to many BSM models

Chronology of μ and τ CLFV searches

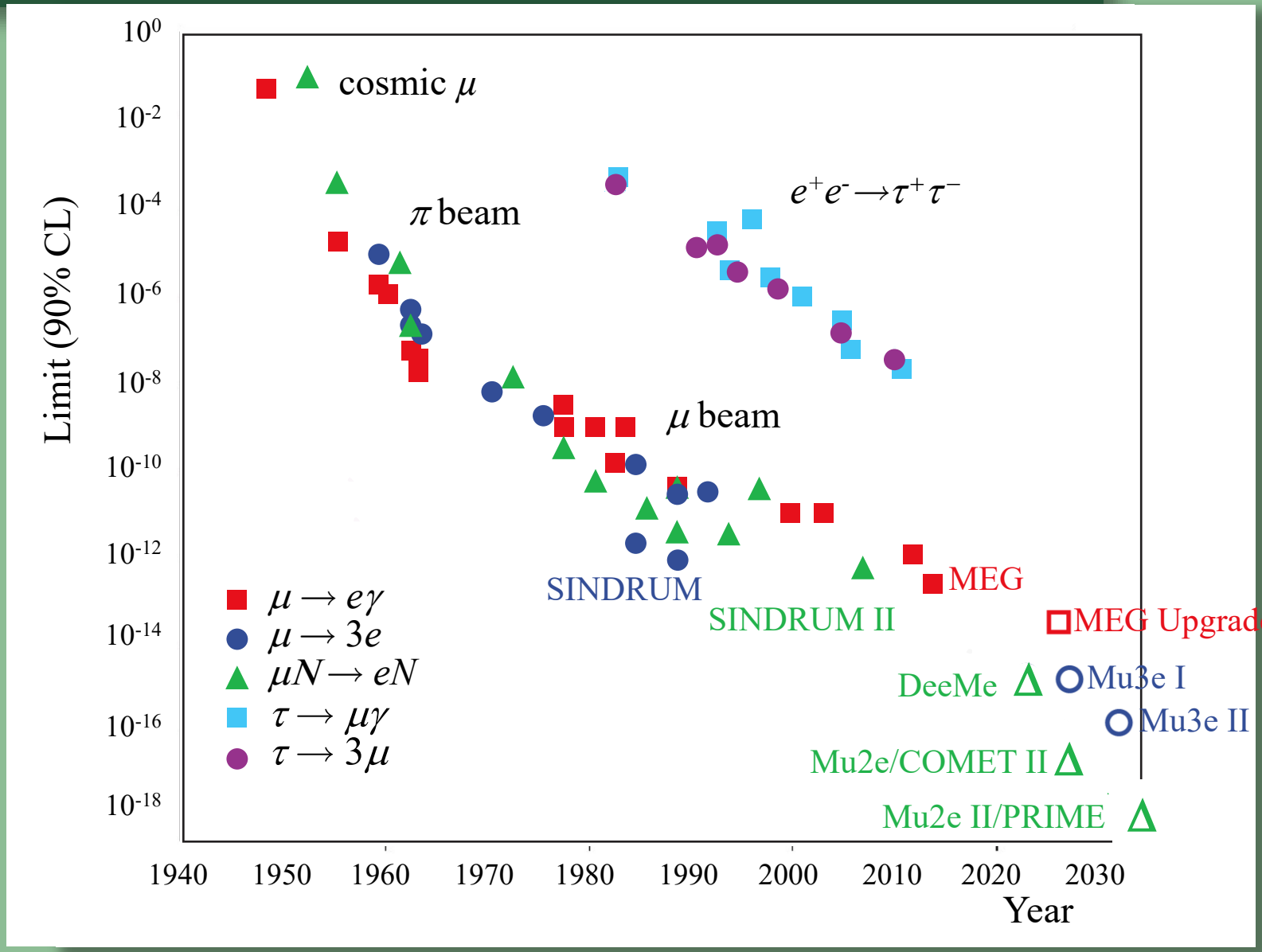

Limits on CLFV τ decays

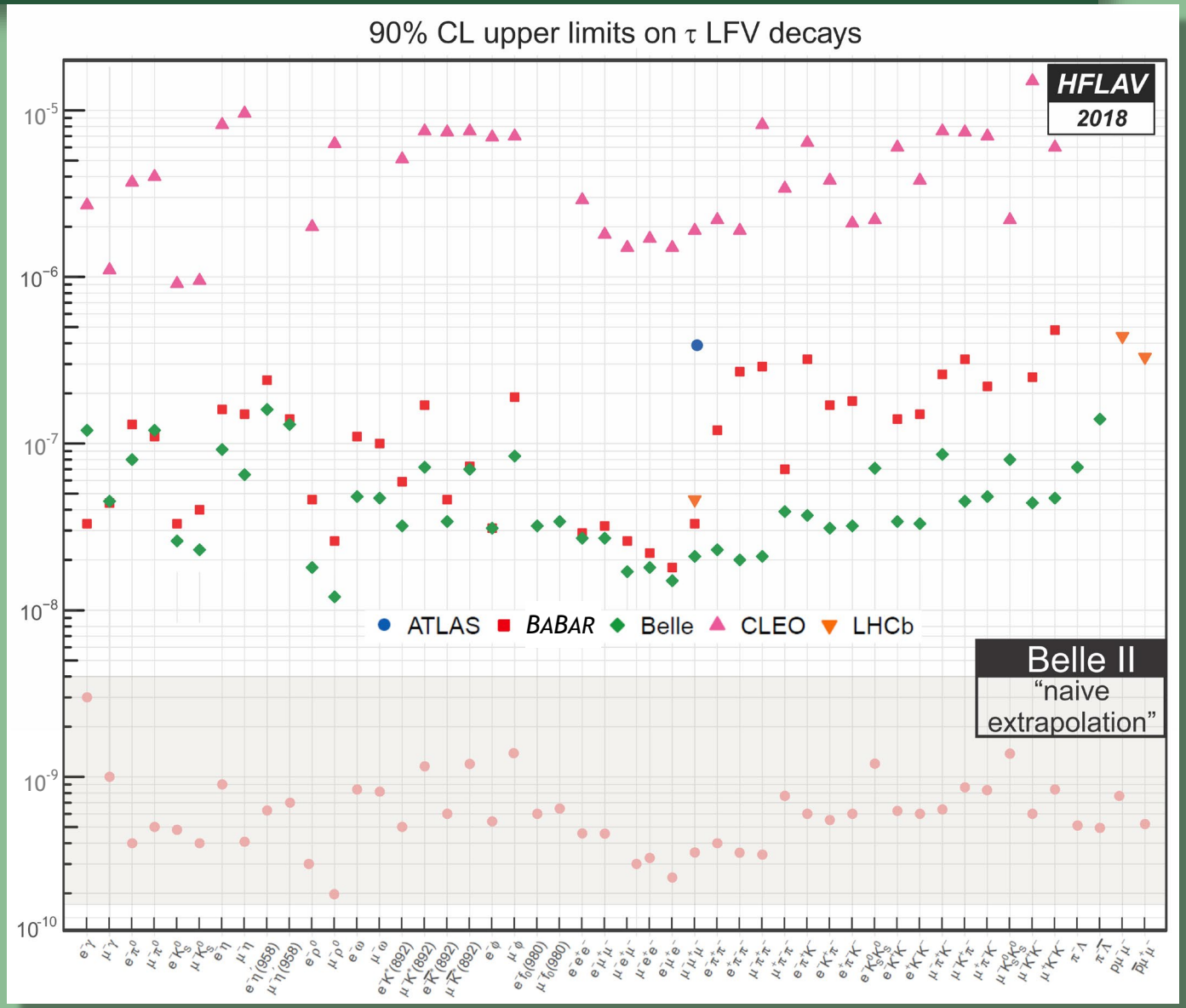

Belle II τ CLFV limits

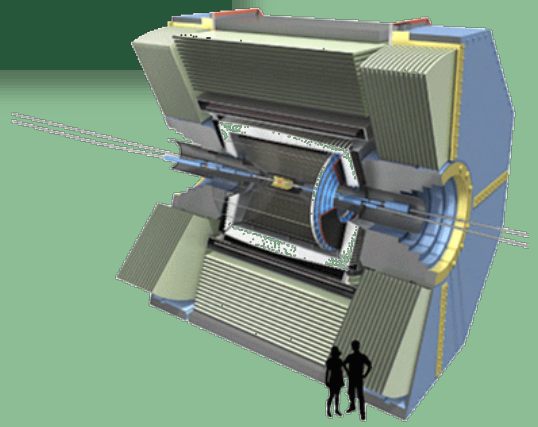

- The target integrated luminosity of 50 ab^{-1} (~5x10^{10} $\tau\bar{\tau}$) will be reached in ~~2025~~ 2031
- The improvement in sensitivity to CLFV τ decays depends on whether or not a particular mode has backgrounds
  - *e.g.*, limits on $\mathcal{B}(\tau\to\ell\ell\ell)$ improve as $1/\int\mathcal{L}dt$ if there is no background, but more slowly, as ~ $1/\int\mathcal{L}dt^{1/2}$, if there is background

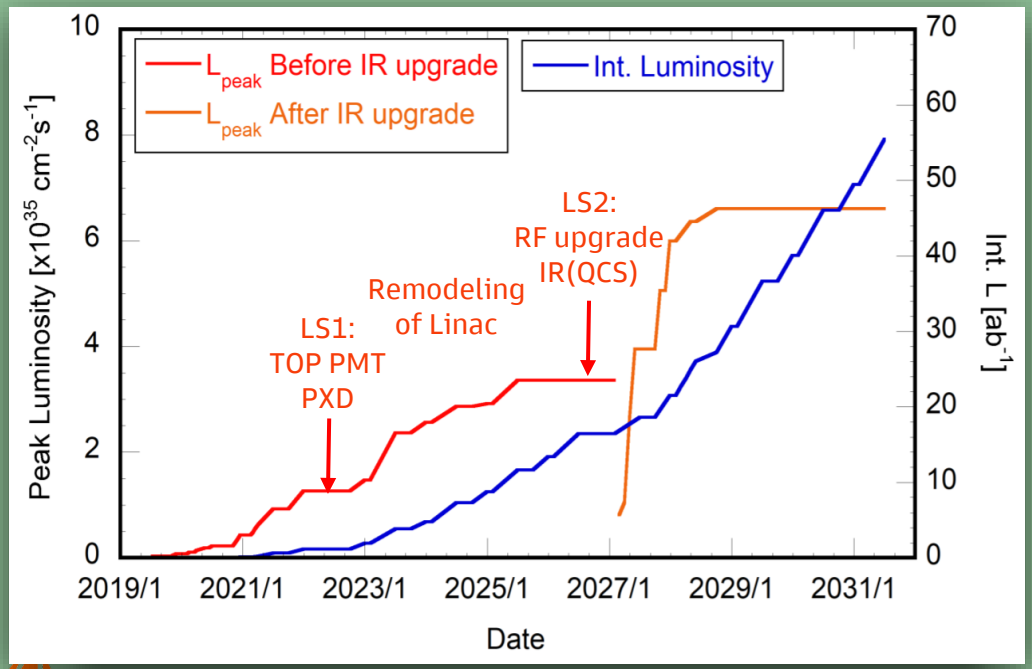

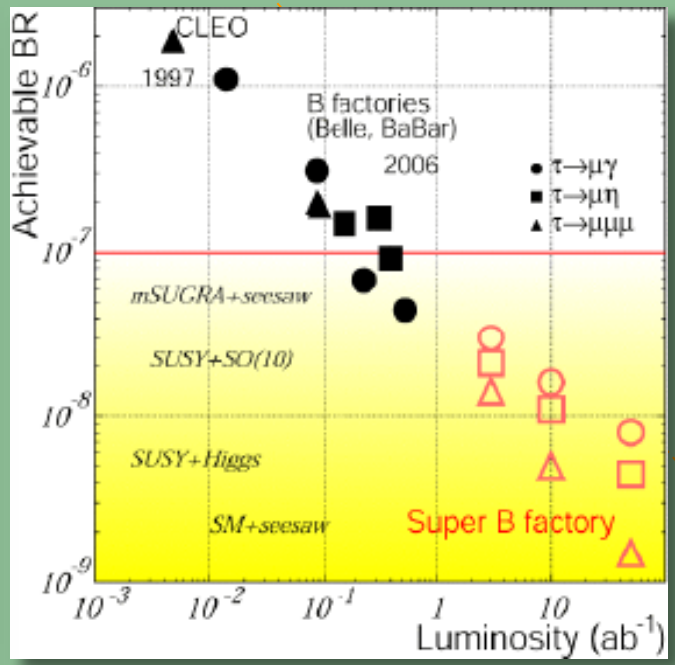

Belle II τ CLFV limits

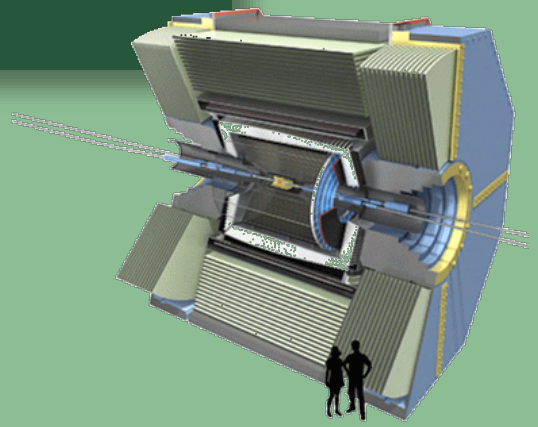

- The target integrated luminosity of 50 ab^{-1} (~5x10^{10} $\tau\bar{\tau}$) will be reached in ~~2025~~ 2031
- The improvement in sensitivity to CLFV τ decays depends on whether or not a particular mode has backgrounds
  - *e.g.*, limits on $\mathcal{B}(\tau\to\ell\ell\ell)$ improve as $1/\int\mathcal{L}dt$ if there is no background, but more slowly, as ~ $1/\int\mathcal{L}dt^{1/2}$, if there is background

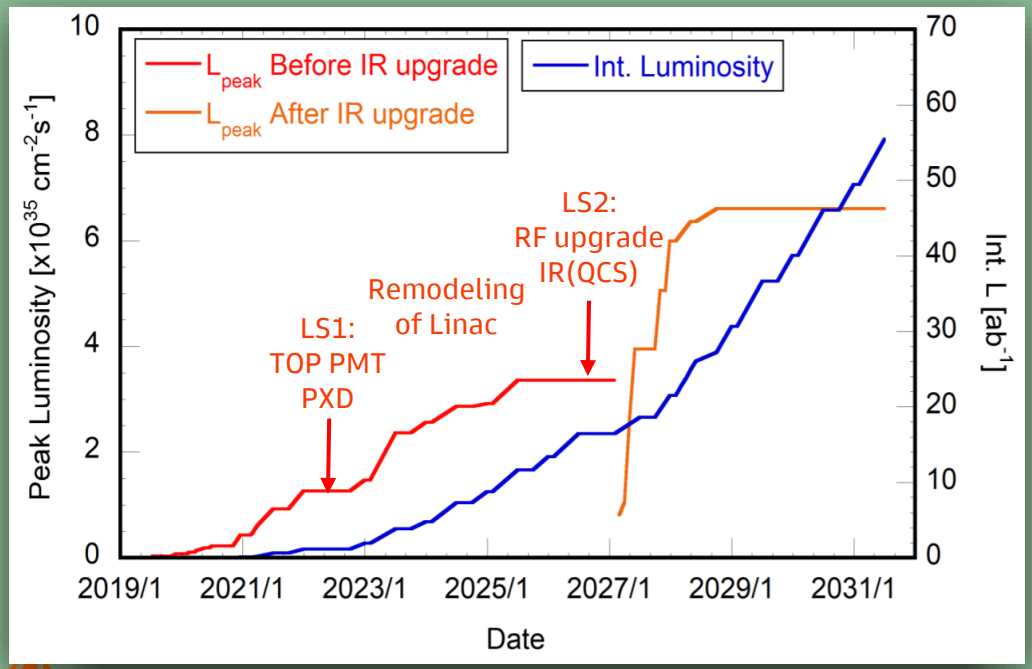

1 ab^{-1} Belle II detector

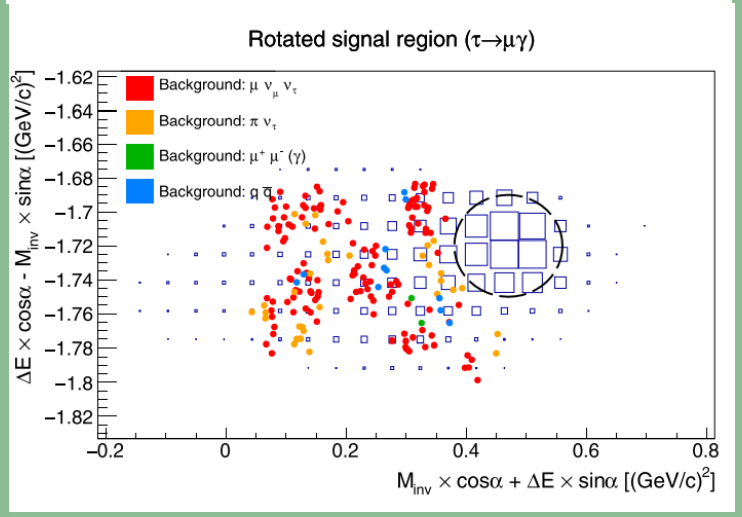

Backgrounds: the name of the game

- At the sensitivities required to advance the state of the art in both τ decays and muon experiments, the primary issue is control of backgrounds in a high rate environment
  - Irreducible backgrounds
  - Accidental backgrounds
- Problematic backgrounds are specific to the type of experiment
- Handles on background control are
  - Charged particle energy resolution
  - Neutral energy resolution
  - Time resolution
  - Particle identification
  - Prompt beam particle rejection
  - Cosmic ray rejection

New muon experiments
- MEG II
- Mu3e
- DeeMe, Mu2e, COMET

New τ decay experiments
Belle II
LHCb

Higgs decay experiments
ATLAS
CMS

Muon experiments: CW *vs* pulsed beams

- **Muon decay** experiments $\mu \to e\gamma$, $\mu \to eee$ use a continuous μ^+ beam, such as the PSI synchrocyclotron surface muon beam
- The dominant backgrounds come from accidental coincidences of two decays
  - background $\propto$ (rate)^2
  - signal $\propto$ rate

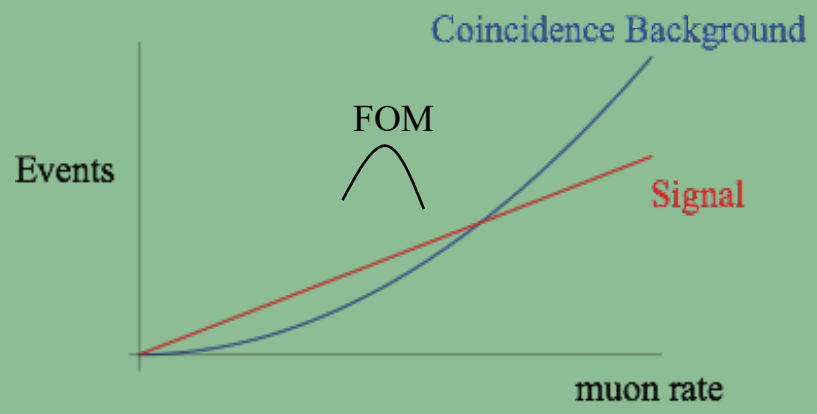

CW operation optimizes the S/N

- $\mu \to e$ **conversion** experiments use a pulsed μ^- beam, such as FNAL or J-PARC
  - There are many prompt pion-induced backgrounds immediately after the proton pulse
  - Use the muon/pion lifetime difference to reduce background

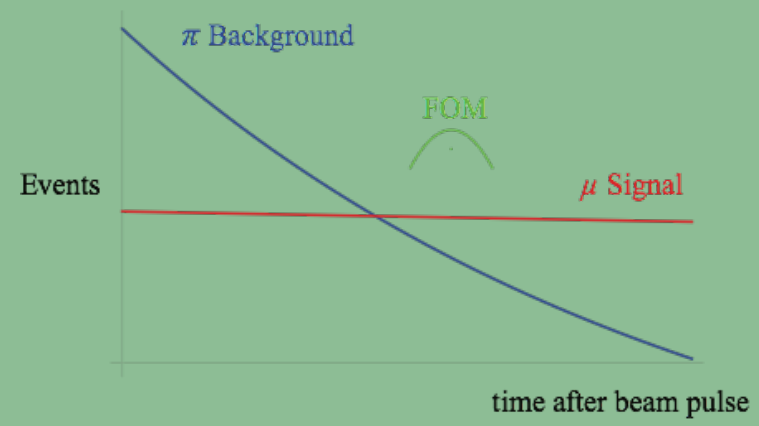

Pulsed operation optimizes the S/N

Muon experiments: CW *vs* pulsed beams

- **Muon decay** experiments $\mu \to e\gamma$, $\mu \to eee$ use a continuous μ^+ beam, such as the PSI synchrocyclotron surface muon beam
- The dominant backgrounds

- $\mu \to e$ **conversion** experiments use a pulsed μ^- beam, such as FNAL or J-PARC
  - There are many prompt pion-induced backgrounds immediately after the

on lifetime
uce

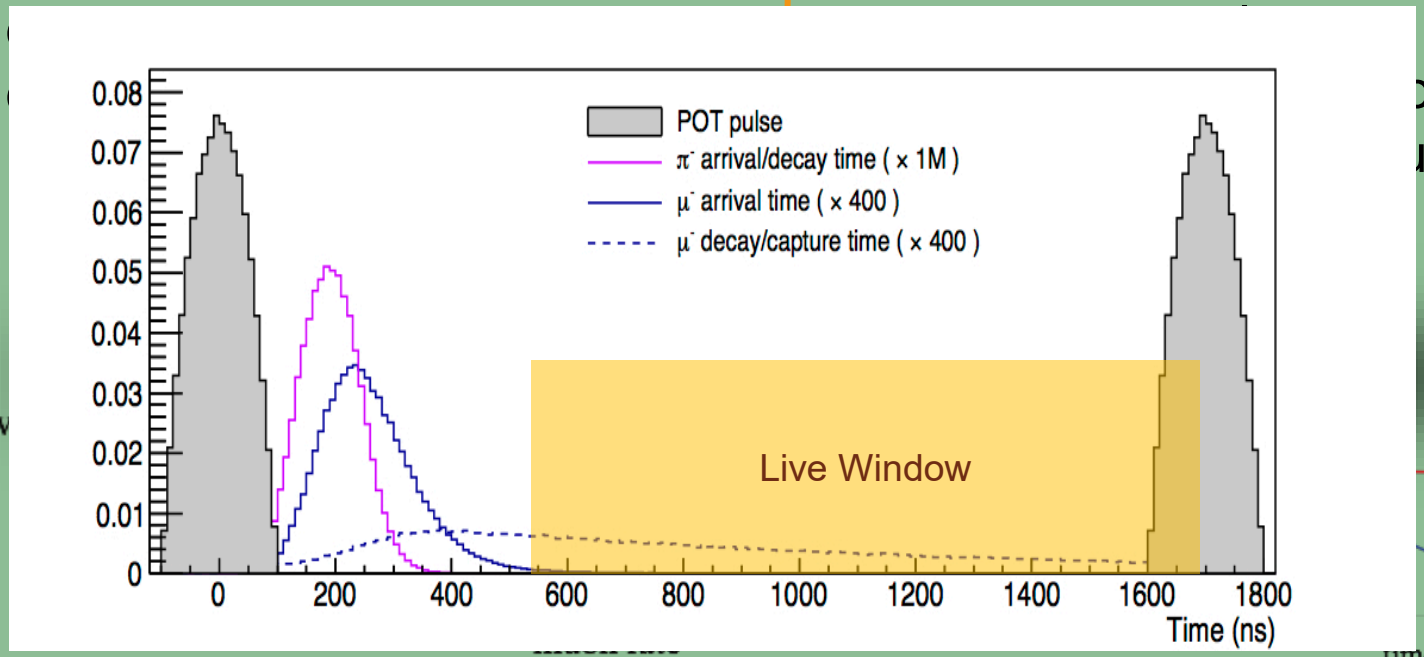

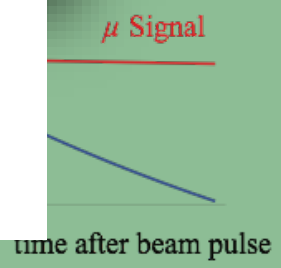

CW operation optimizes the S/N

Pulsed operation optimizes the S/N

$\mu \to e\gamma$ signal and backgrounds

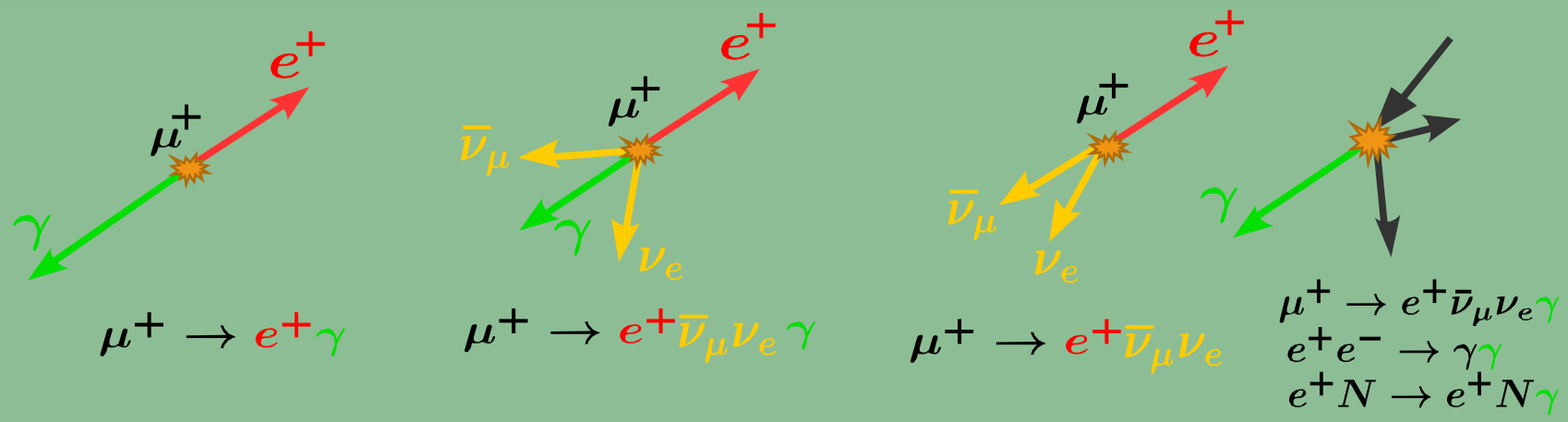

CLFV signal $\propto R_\mu$

Radiative muon decay correlated $\propto R_\mu$

Accidental background uncorrelated $\propto R_\mu^2$

Events are described by five variables: $E_\gamma, E_e, t_{e\gamma}, \theta_{e\gamma}, \phi_{e\gamma}$

MEG at PSI

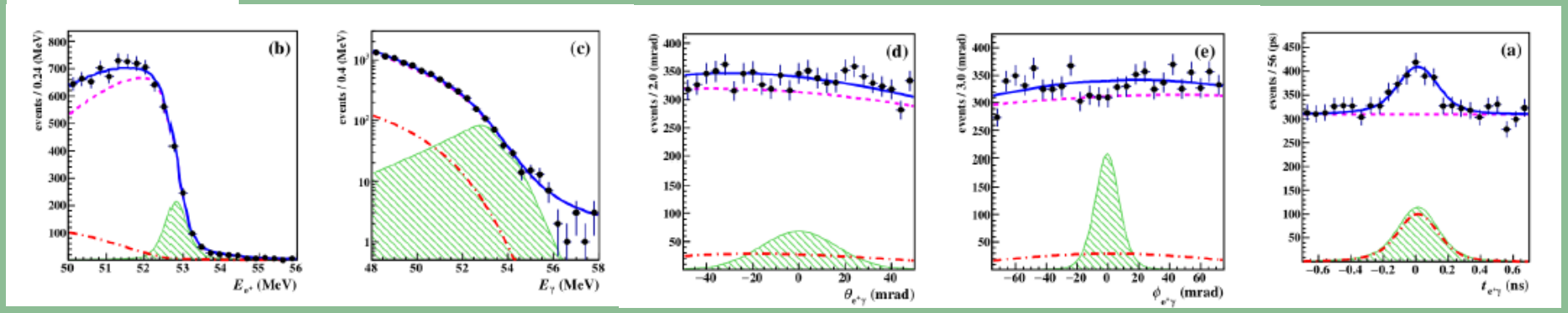

MEG backgrounds

- Backgrounds are dominated by accidental coincidences from
  $\mu \to e\nu\nu\gamma \sim (1 - 2E_\gamma/m_\mu)$ $\Gamma_{acc} \propto \Gamma_\mu^2 \cdot \varepsilon_e \cdot \varepsilon_\gamma \cdot \delta E_e \cdot \left(\delta E_\gamma\right)^2 \cdot \left(\delta\theta_{e\gamma}\right)^2 \cdot \delta t_{e\gamma}$
- These considerations dictated the original MEG design and the improvements incorporated in the upgrade

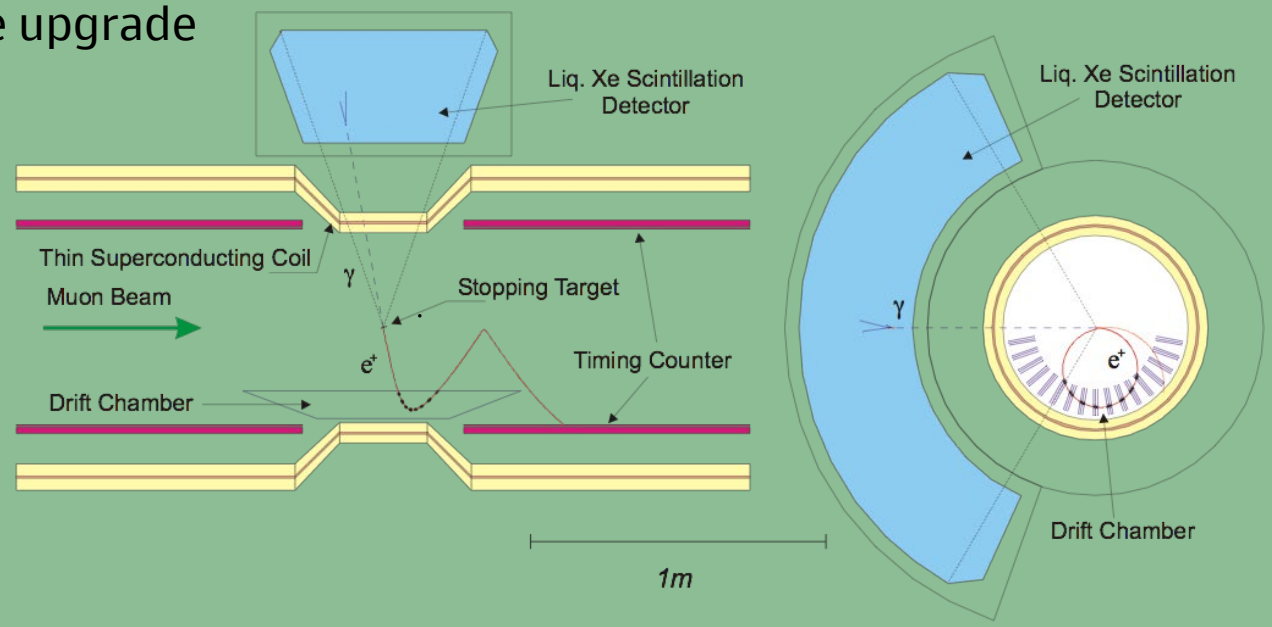

- MEG employed a DC surface muon beam: $|p_\mu|$ 28 MeV/c, 3×10^7 μ stops/s
- With a total of 7.5×10^{14} stopped muons, gathered in runs from 2009 - 2013 MEG set a 90% CL limit of $< 4.2 \times 10^{-13}$ (Baldini *et al.*, Eur.Phys.J. C76434, 2016)

MEG II – 2x resolution improvement

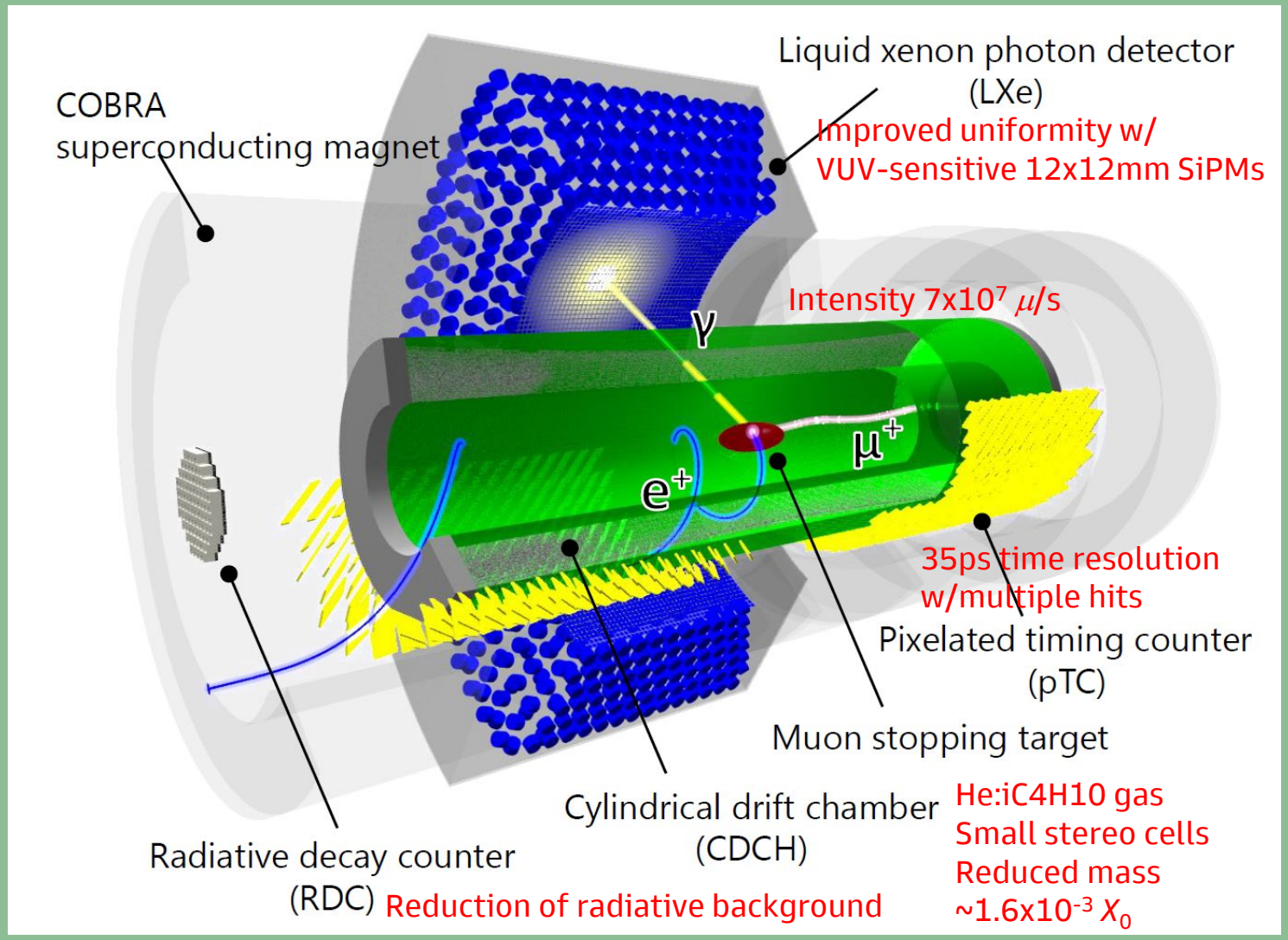

MEG upgrade – 2x resolution improvement

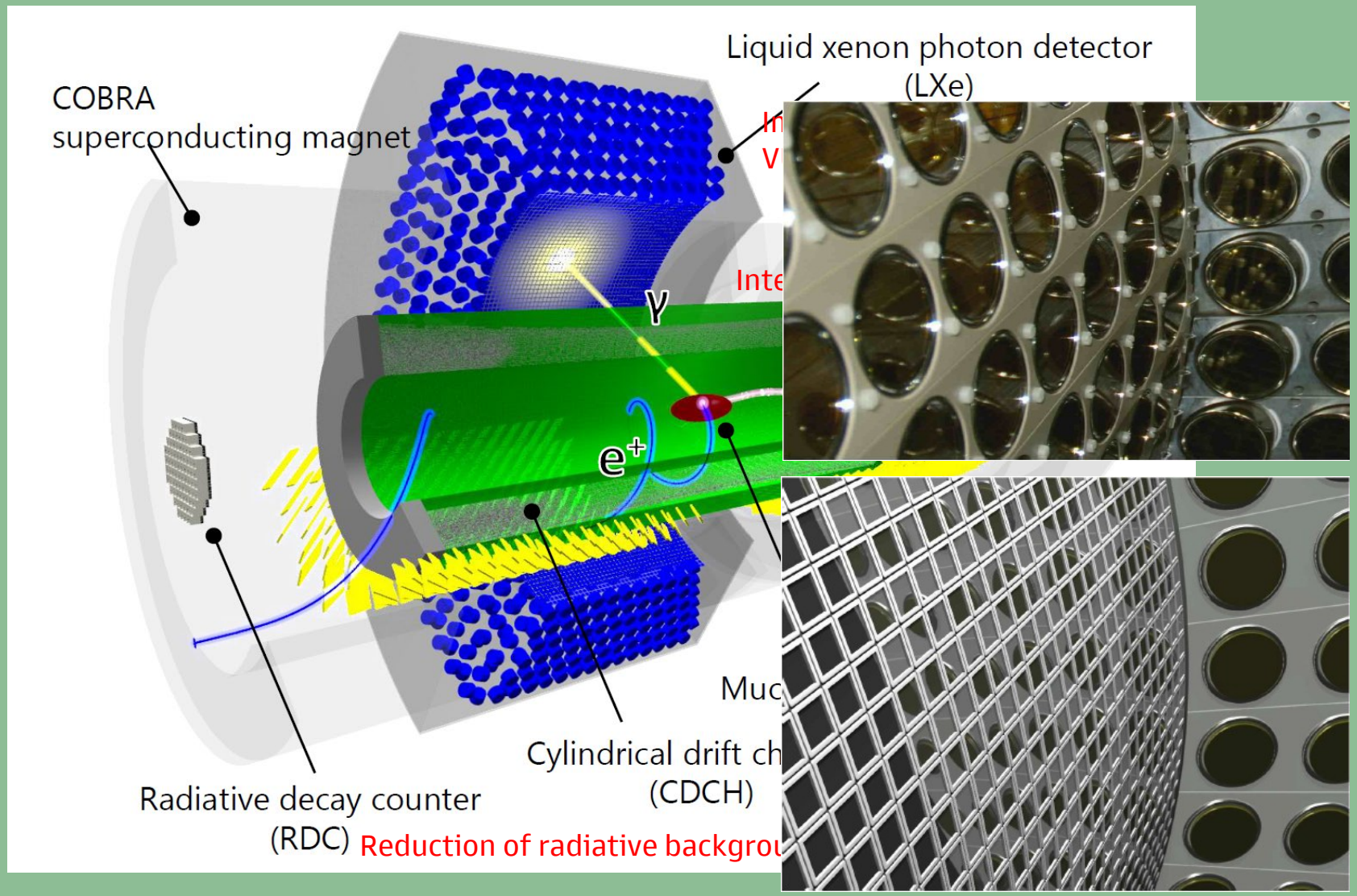

MEG II status

- The MEG II Upgrade improves the detector (2x improvements in resolution and efficiency) to achieve a 90% CL limit of $\mathcal{O}\, 6 \times 10^{-14}$ in a three year run
- Schedule
  - Commissioning runs in 2017-2020
  - Engineering run in Aug 2021
    - Install full DAQ, electronics
    - Full LXe electronics
    - Degradation of MPPC PDE ($\Rightarrow$limit on μ stops/run),
    - Drift chamber conditioning to reduce corona discharge
      - New chamber to be built by March 2023
    - Physics runs start presently

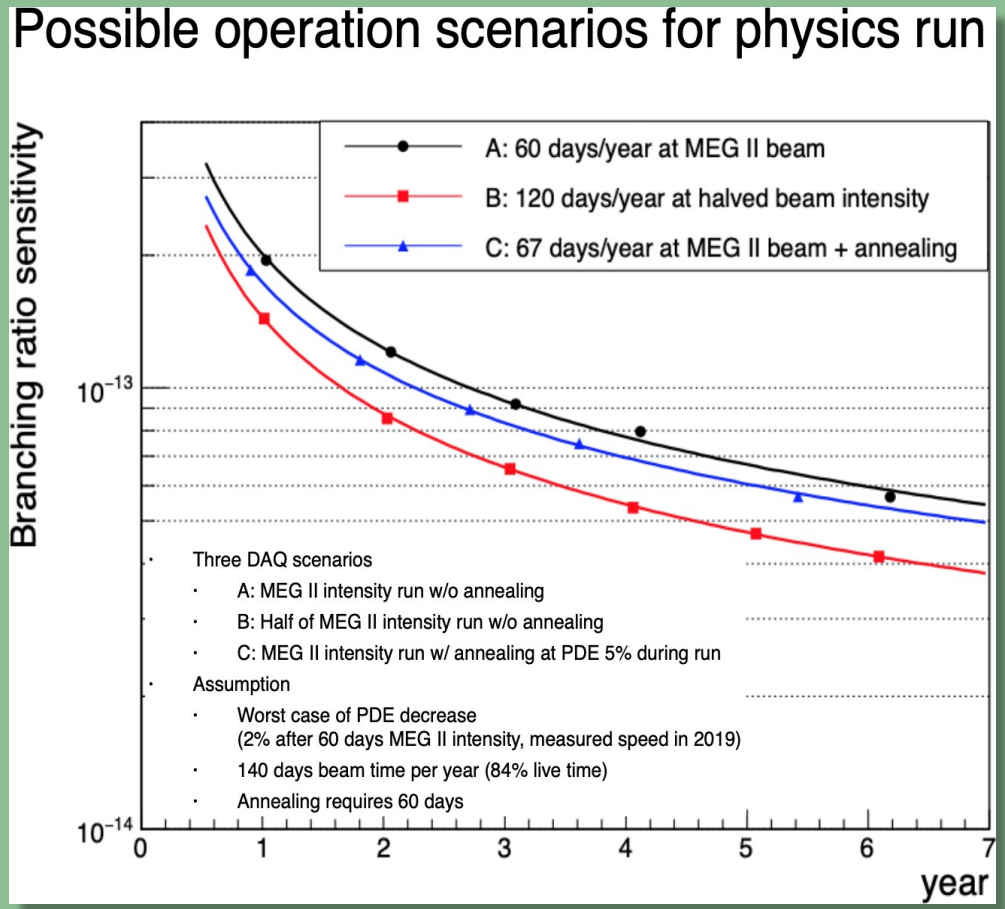

$\mu^+ \rightarrow e^+ e^+ e^-$ $\Rightarrow$ Mu3e at PSI

Signal

$E = m_\mu$
$\Sigma p_i = 0$
Vertex

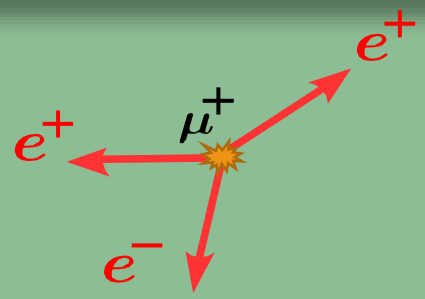

Background

Accidentals

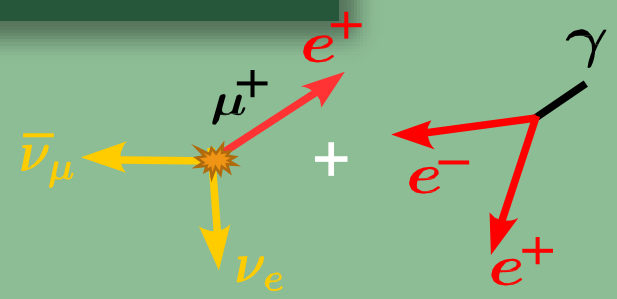

Radiative decay
w internal conversion

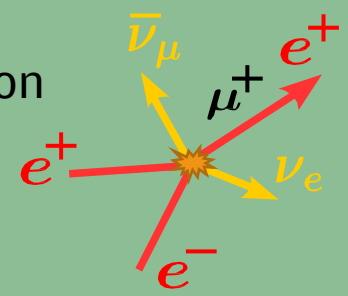

- **Current limit:** 1.0×10^{-12} (SINDRUM at PSI, 1988)
- Mu3e at will provide substantial improvement
  - Uses a surface muon beam - πE5 beamline
  - Phase I
    - ~~2018~~ - 10^8 μ^+/s
    - Sensitivity 10^{-15}
  - Phase II HIMB 10^9 μ^+/s
    - Sensitivity 10^{-16}

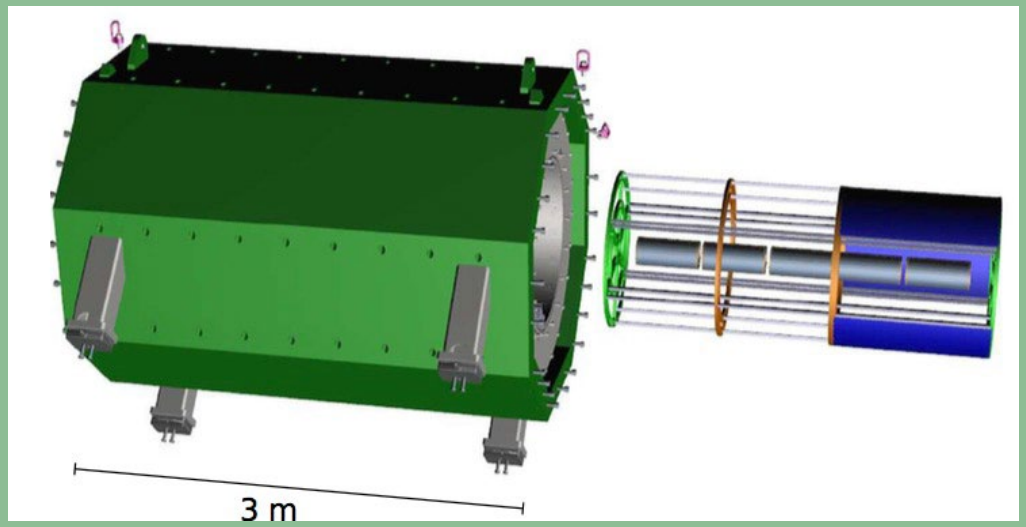

Mu3e detail

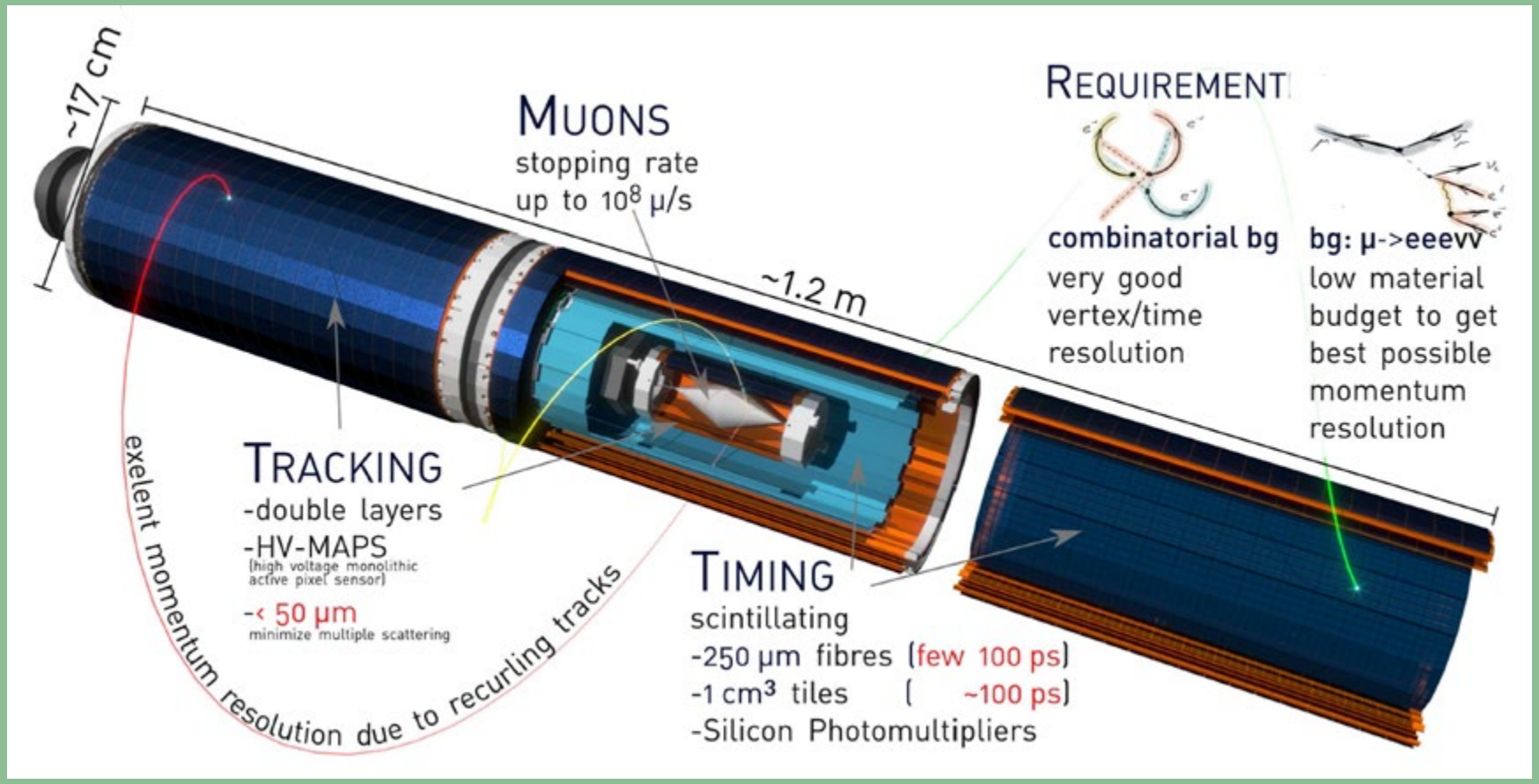
~17 cm
MUONS
stopping rate
up to 10^8 μ/s
~1.2 m
REQUIREMENT
combinatorial bg
very good
vertex/time
resolution
bg: μ->eeeνν
low material
budget to get
best possible
momentum
resolution
TRACKING
-double layers
-HV-MAPS
(high voltage monolithic
active pixel sensor)
-< 50 μm
minimize multiple scattering
exelent momentum resolution due to recurling tracks
TIMING
scintillating
-250 μm fibres (few 100 ps)
-1 cm³ tiles (~100 ps)
-Silicon Photomultipliers

$\mu^+ \rightarrow e^+ e^+ e^-$ ⇒ Mu3e at PSI

Signal

$E = m_\mu$
$\Sigma p_i = 0$
Vertex

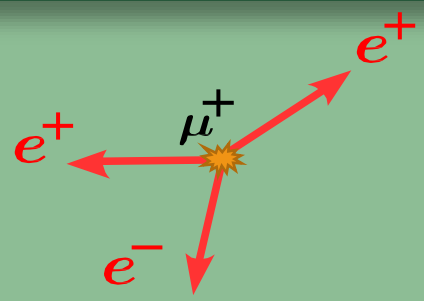

Background

Accidentals

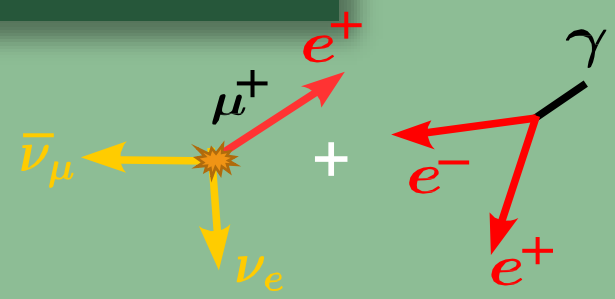

Radiative decay
w internal conversion

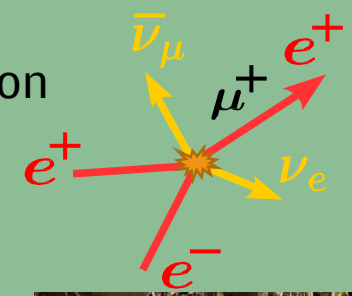

- **Current limit:** 1.0×10^{-12} (SINDRUM at PSI, 1988)
- Mu3e will provide substantial improvement
  - Uses a surface muon beam - πE5 beamline
  - Phase I
    - ~~2018~~ - 10^8 μ^+/s
    - Sensitivity 10^{-15}
  - Phase II HIMB 10^9 μ^+/s
    - Sensitivity 10^{-16}
- Mu3e had an integration run in the πE5 beam line from May to July 2021 with a reduced detector: 2 pixel layers + fiber detector inserted into the magnet

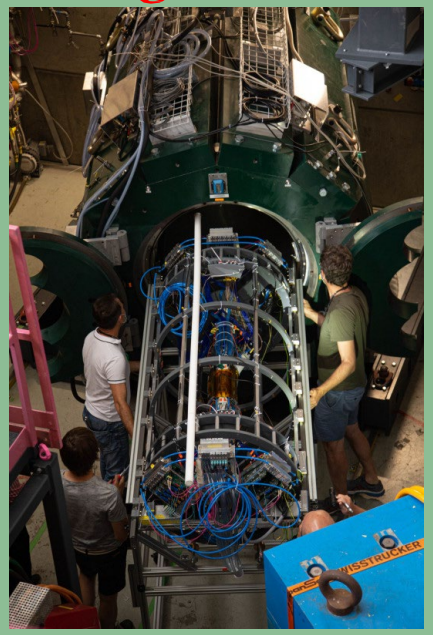

Mu3e sensitivity

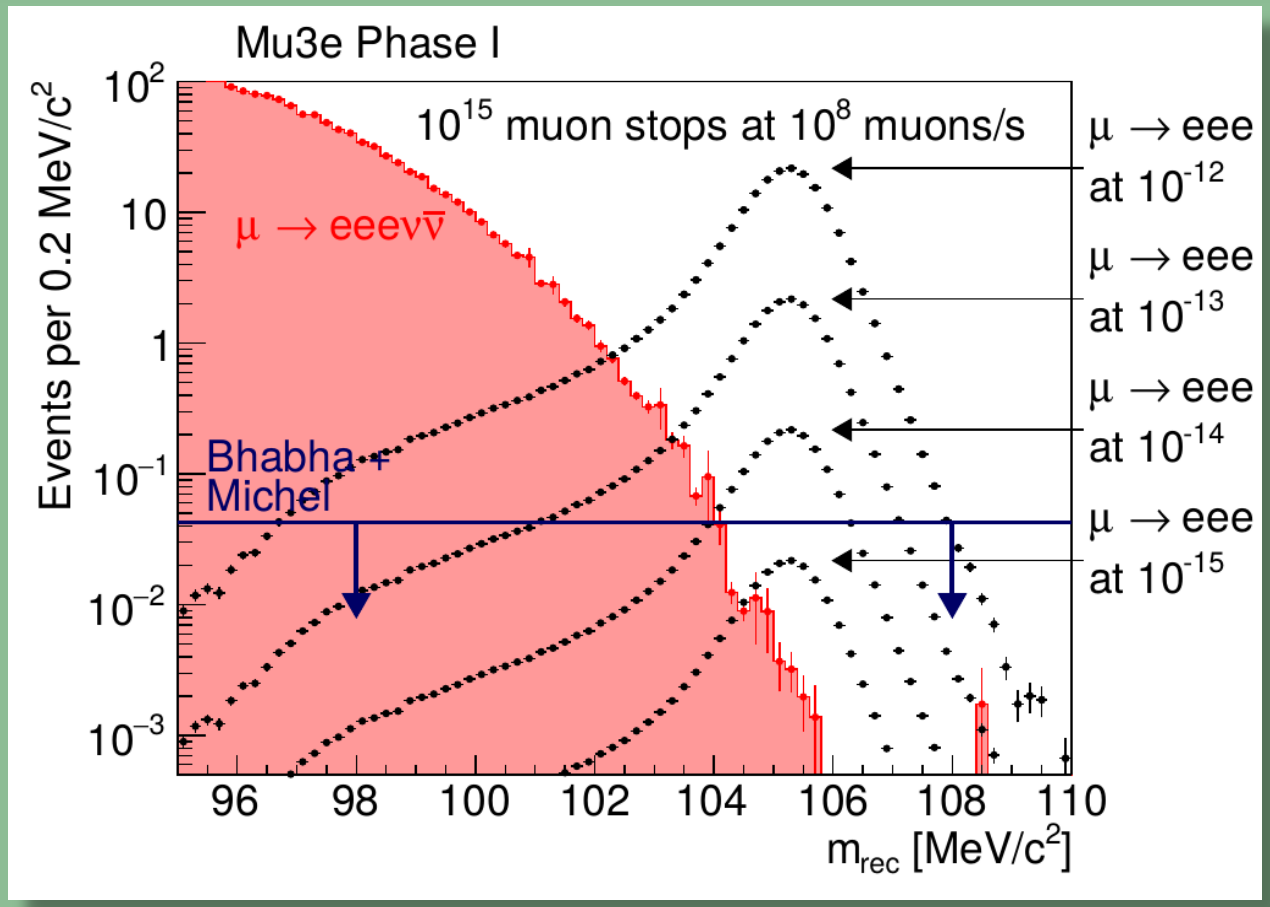

Mu3e sensitivity

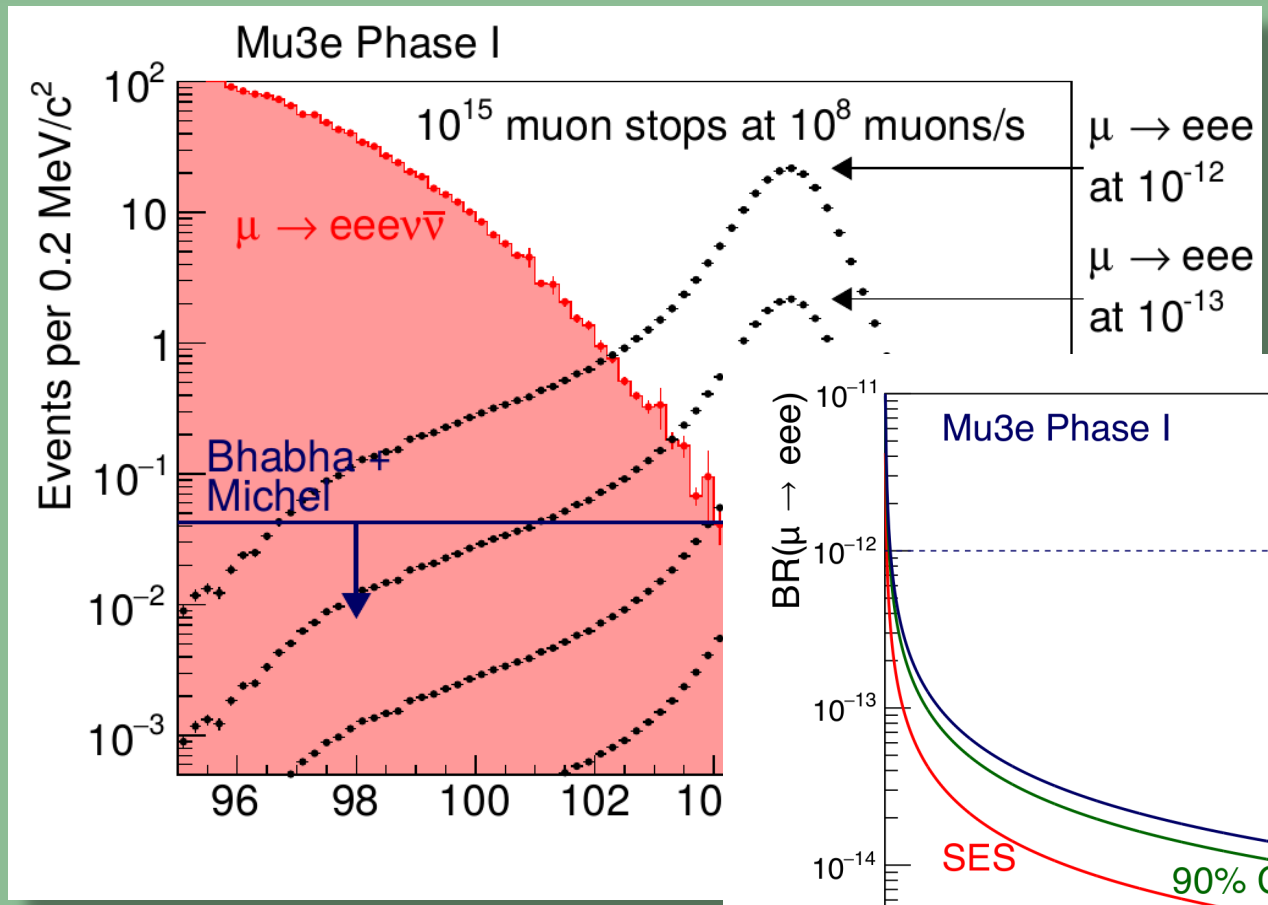

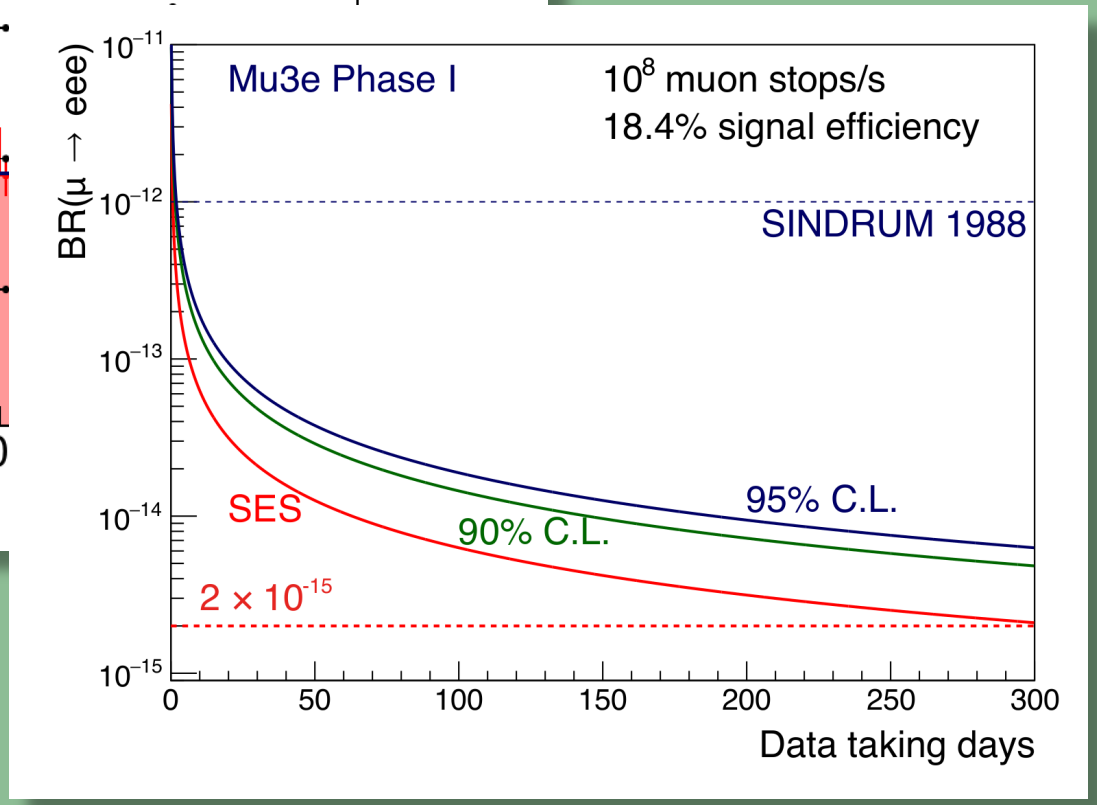

μ to e conversion experiments

- The signal is a single mono-energetic electron
- If N = Al, E_e ~105 MeV
  - electron energy depends on Z, due to atomic binding energy
- Coherent nuclear recoil
- There are three experiments in various stages of preparation
  - DeeMe
  - COMET Phase I and Phase II
  - Mu2e

  } Origins trace to MELC and MECO proposals
    - All face similar challenges, addressed in specific ways
      - High rates to achieve required sensitivity
      - Prompt and delayed beam-related backgrounds
      - Cosmic ray backgrounds
  - PRISM/Prime is a muon storage ring based accelerator/detector concept

$$R_{\mu e} = \frac{\Gamma(\mu^- + N(A,Z) \rightarrow e^- + N(A,Z))}{\Gamma(\mu^- + N(A,Z) \rightarrow \text{all muon captures})}$$

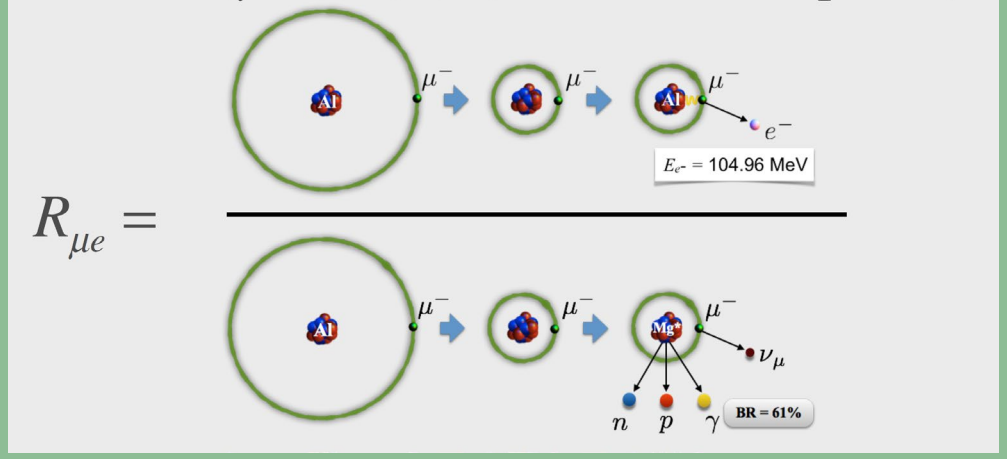

Decay-in-Orbit Shape

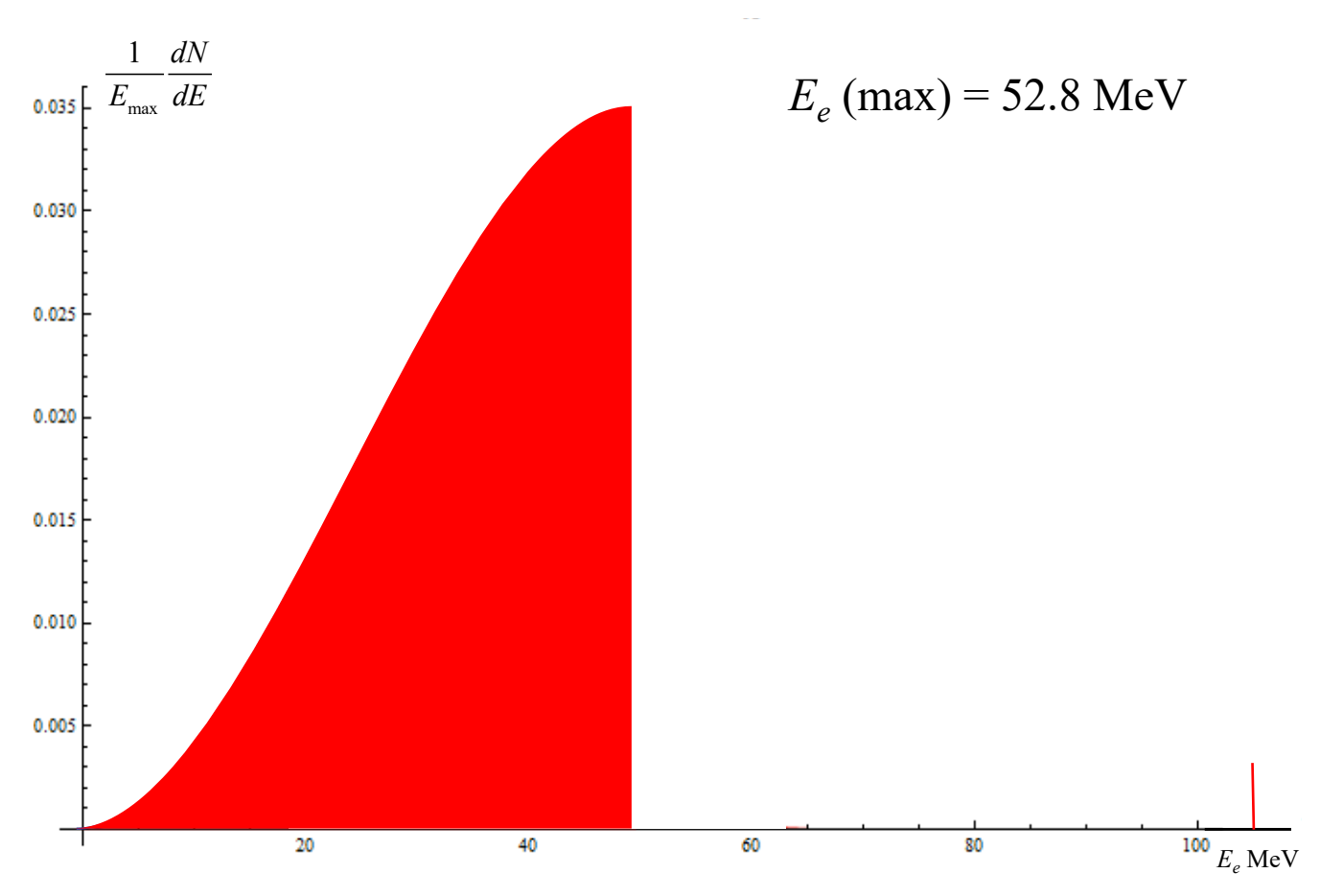

Decay-in-Orbit Shape

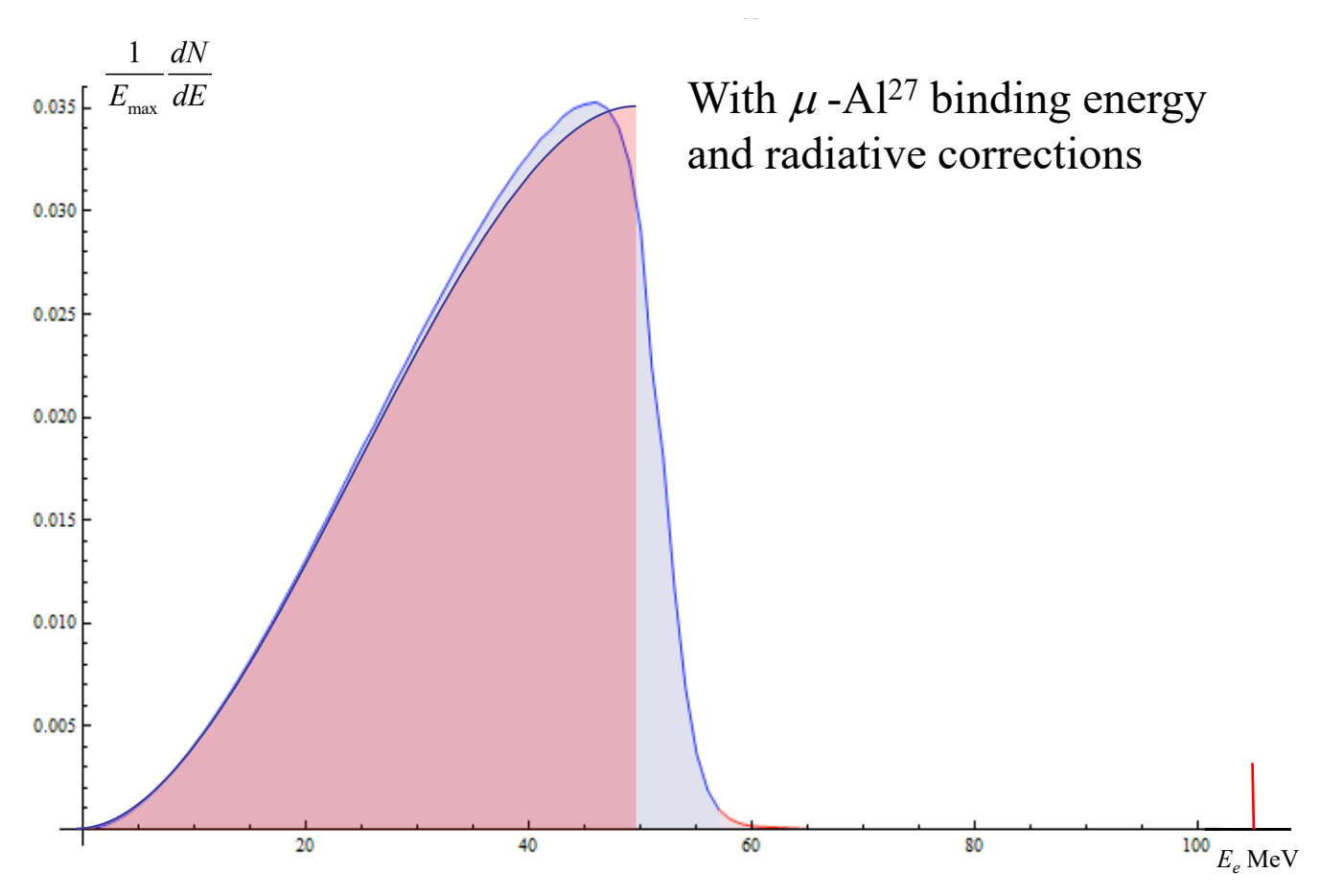

Czarnecki
Szafron

Decay-in-Orbit Shape

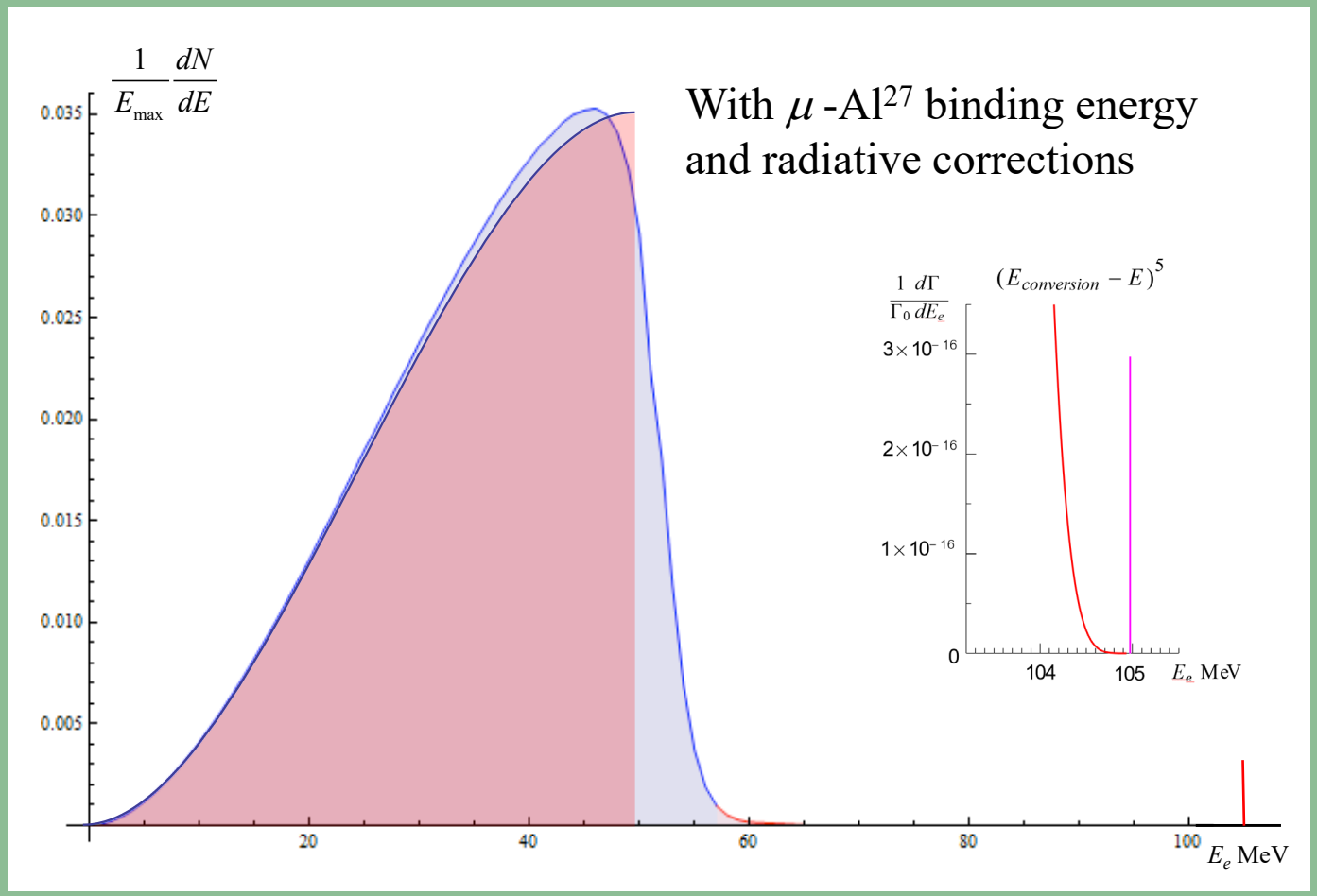

Czarnecki
Szafron

DeeMe at JPARC

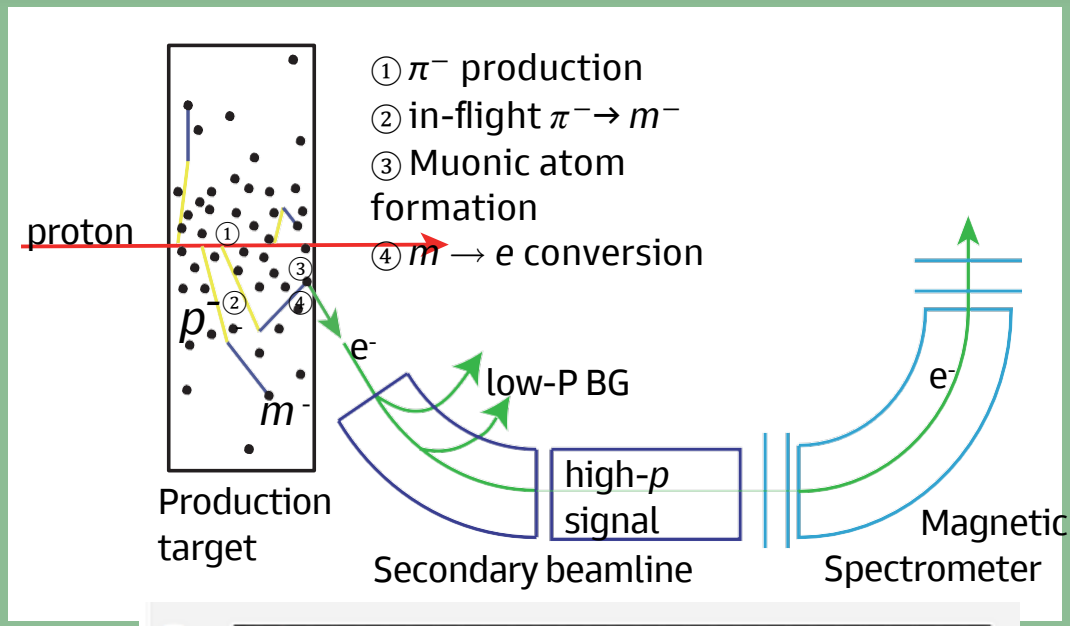

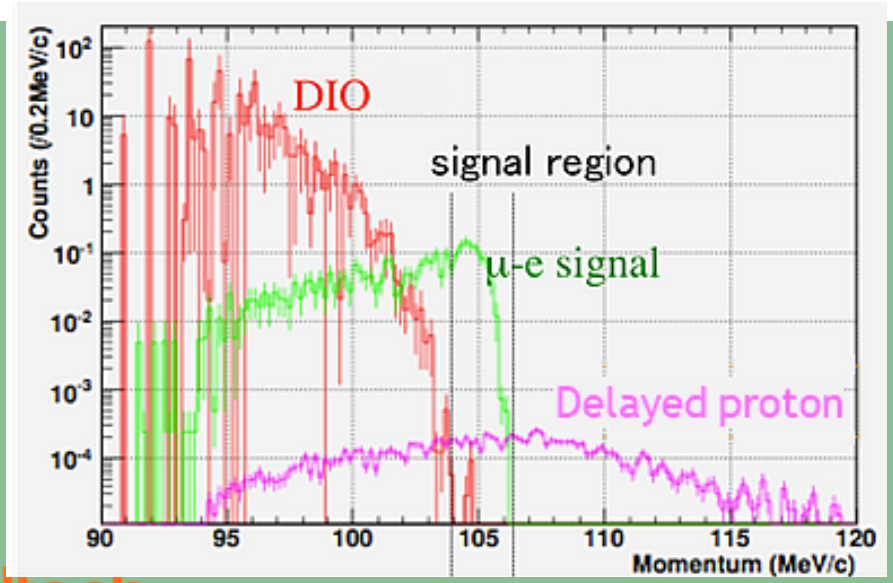

$\mu N \rightarrow eN$

Novel Idea: μ-e conversion in the primary production target

Signal is a delayed single mono-energetic electron identified by measuring its momentum in spectrometer using Pac-Man magnet from TRIUMF

Beamline shared with other experiments (g-2)

DeeMe at JPARC

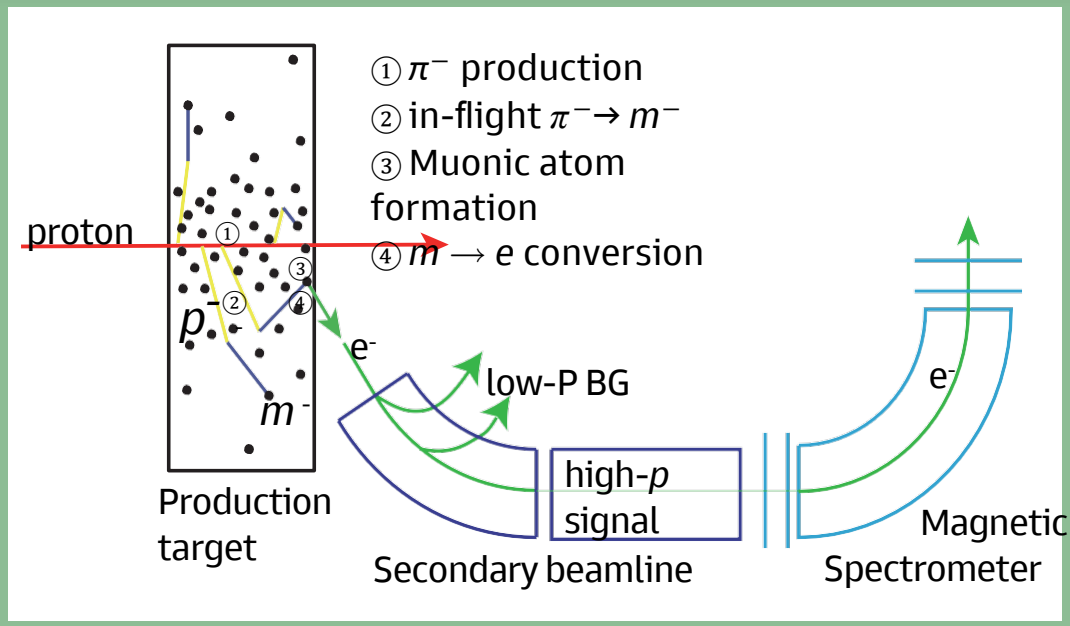

$\mu N \rightarrow eN$

Novel Idea: μ-e conversion in the primary production target

Signal is a delayed single mono-energetic electron identified by measuring its momentum in spectrometer using Pac-Man magnet from TRIUMF

Beamline shared with other experiments (g-2)

Start with carbon target

- Lifetime of muonic atom ~2μs
- Energy of electron from $\mu \rightarrow e$ conversion = 105 MeV
- Single event sensitivity (1 year = 2×10^7 sec)
  - 1×10^{-13}
  - 2×10^{-14} (4 years)

Upgrade to SiC

  - 3×10^{-14}
  - 5×10^{-15} (4 years)

DeeMe status

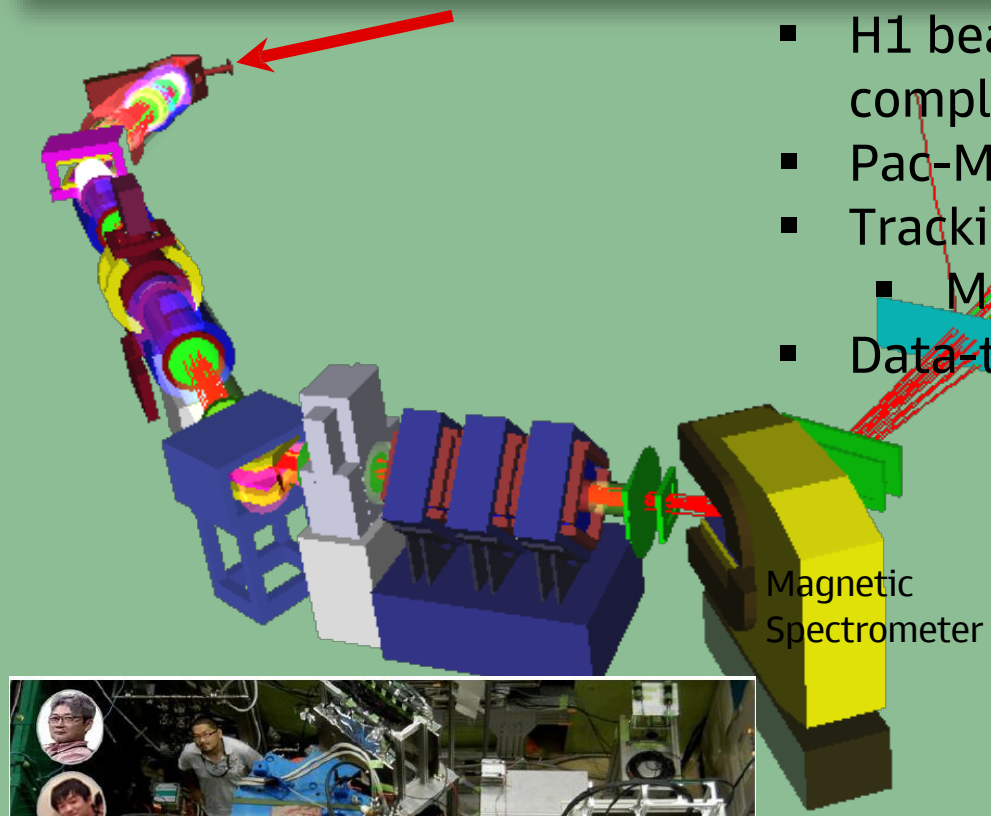

- H1 beamline expected to be completed in Jan 2022
- Pac-Man magnet installed
- Tracking + electronics exists
  - Measured DIO spectrum
- Data-taking to start in 2022

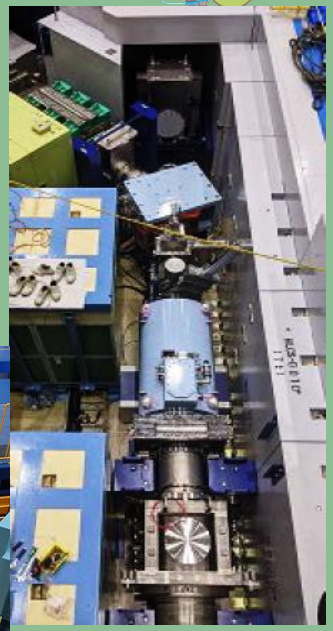

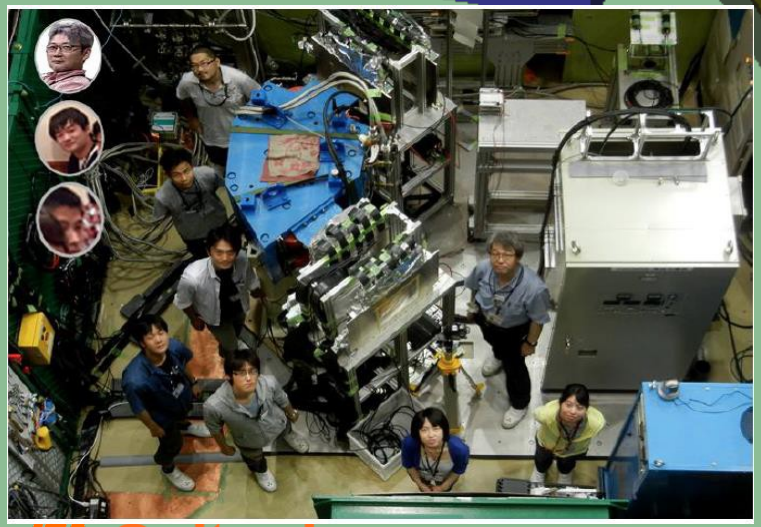

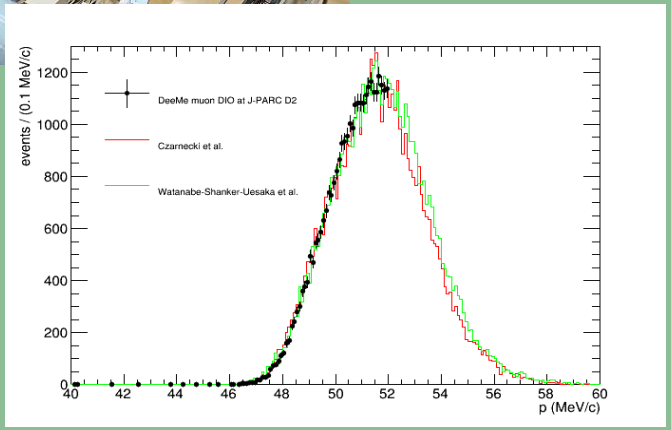

Mu2e

- The Mu2e sensitivity goal 2.6×10^{-17} demands a total of ~ 6×10^{17} stopped muons in a 3 year run of ~ 6×10^{7} seconds total
- This requires a muon stopping rate of 10^{10}/sec

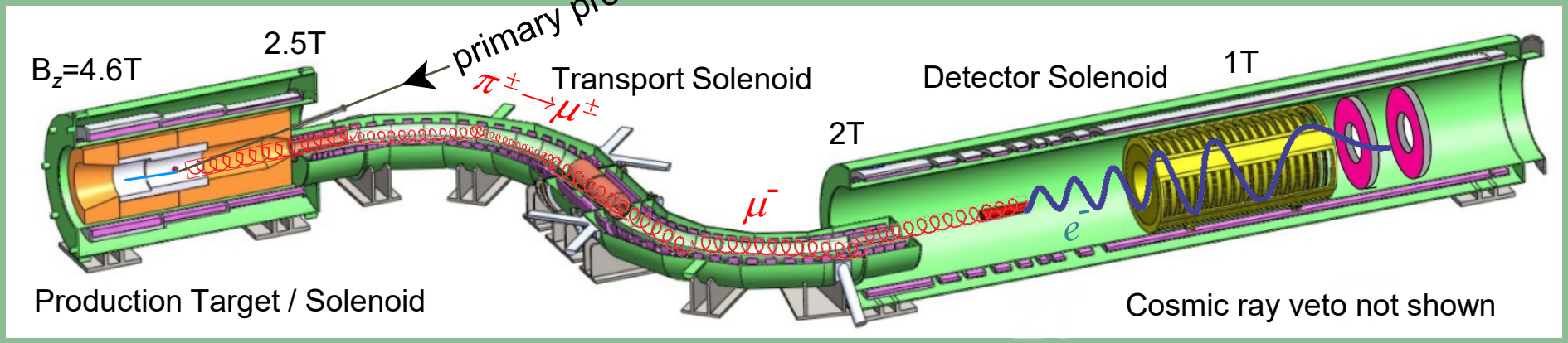

- Experimental design
  - Pulsed proton beam produce pions, which are captured in the backward direction
  - Transport muons from pion decay, with momentum and sign selection
  - Since electron backgrounds are at lower momentum than the sought conversion electrons, confine lower momentum particles to smaller helical radii in a solenoid and a provide hole in tracker and calorimeter for them to pass through
  - Reject cosmic ray events

Cosmic ray veto (four layers)

Covers as much of the transport and detector solenoids as possible
Nonetheless, timing properties of the calorimeter are required to achieve required cosmic ray rejection

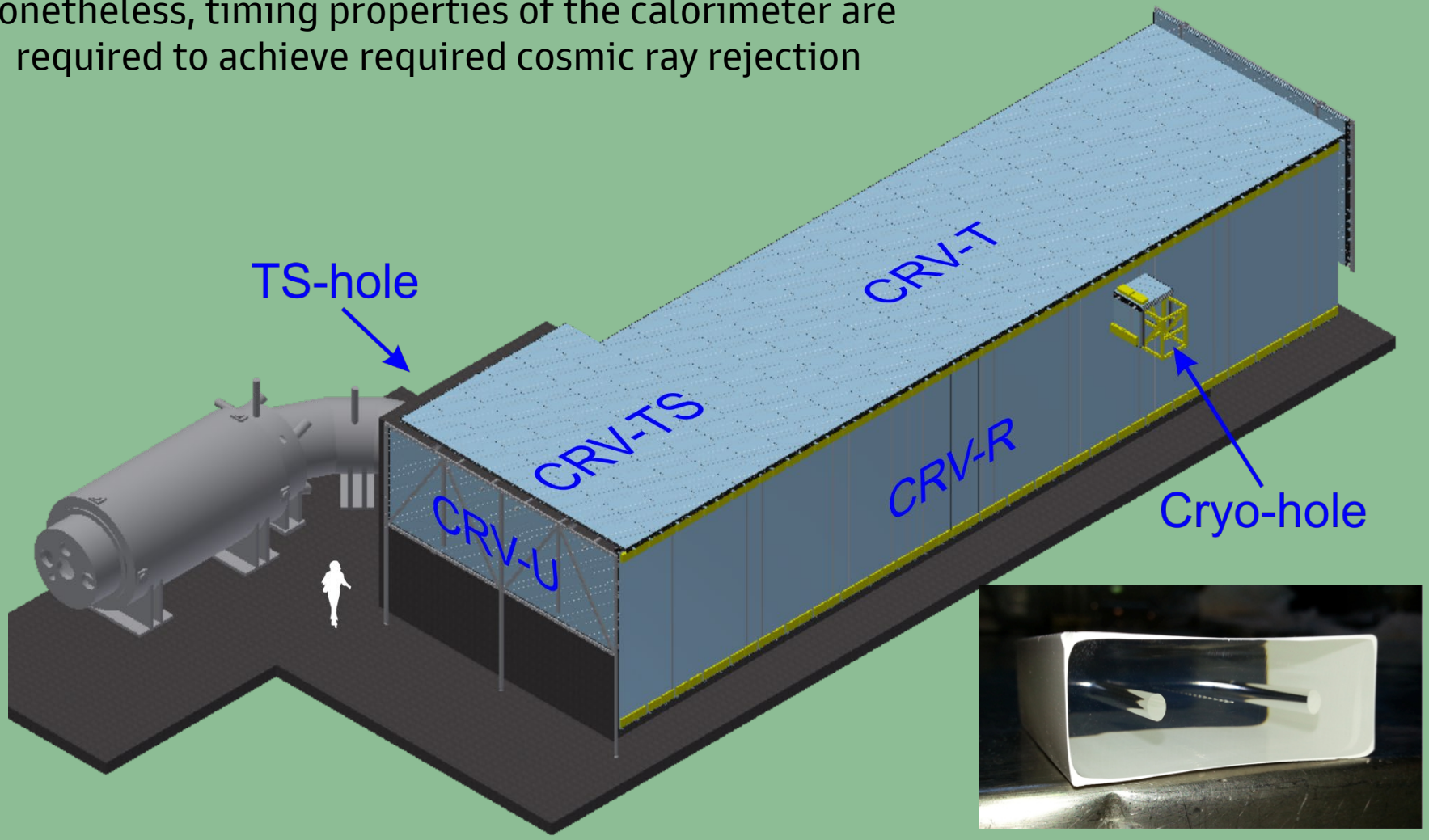

What happens during a microbunch ?

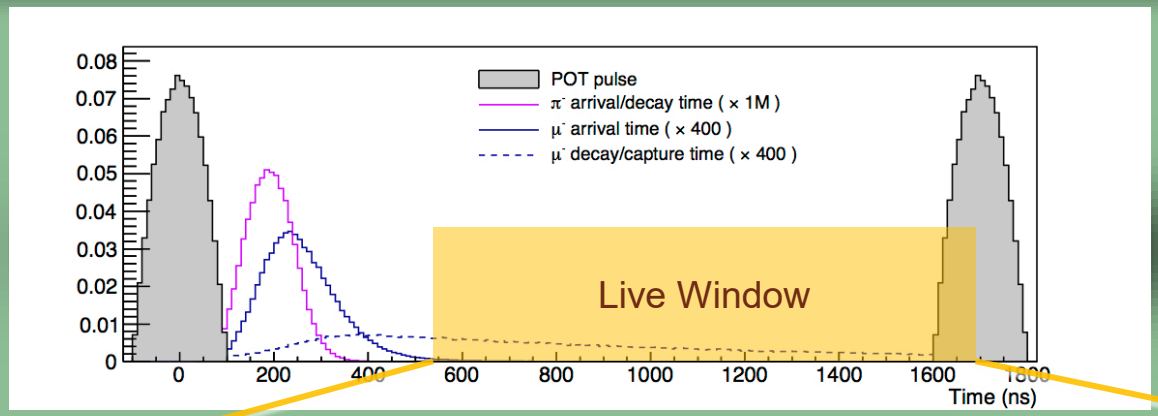

Use of pulsed proton beam and a delayed live gate allows suppression of prompt backgrounds by many orders of magnitude

Proton pulses must be narrow

Out-of-time protons must be suppressed by $\mathcal{O}(10^{10})$

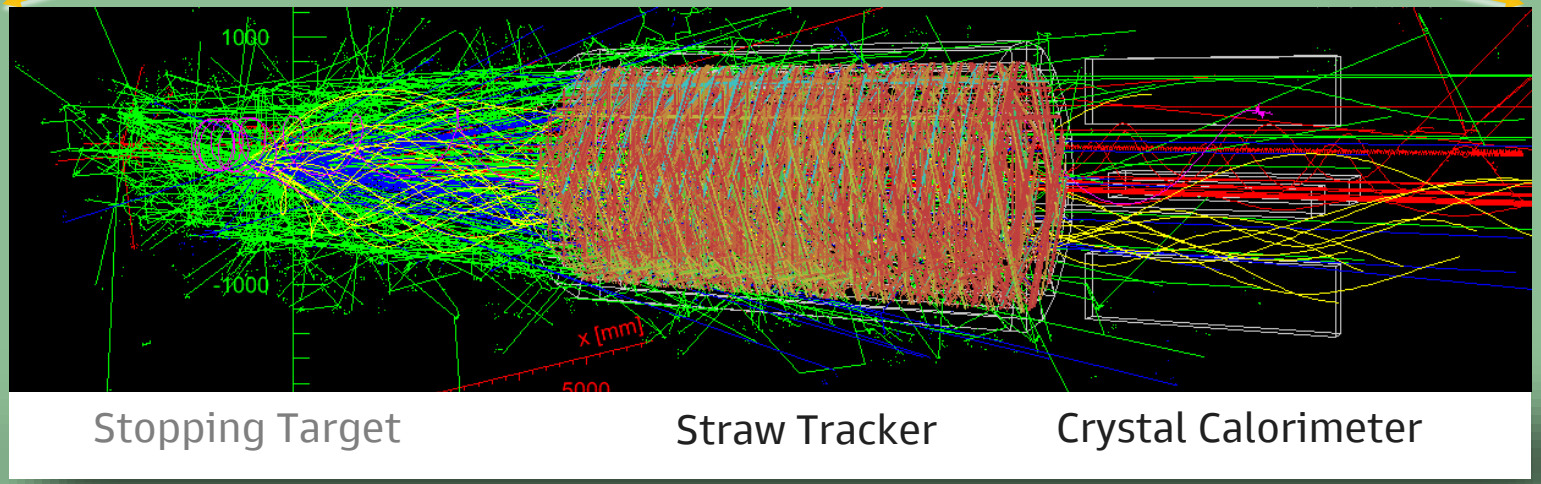

- Simulations encompass a full ~1μs, including all the background overlays from the beam flash, μ capture products, neutrons, *etc*. and properly account for contributions from previous bunches.

What happens during a microbunch ?

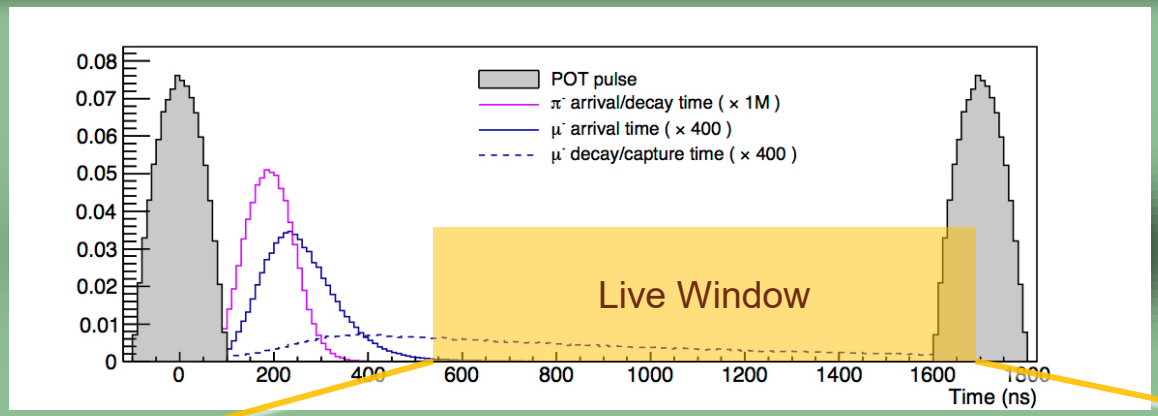

Use of pulsed proton beam and a delayed live gate allows suppression of prompt backgrounds by many orders of magnitude

Proton pulses must be narrow

Out-of-time protons must be suppressed by $\mathcal{O}(10^{10})$

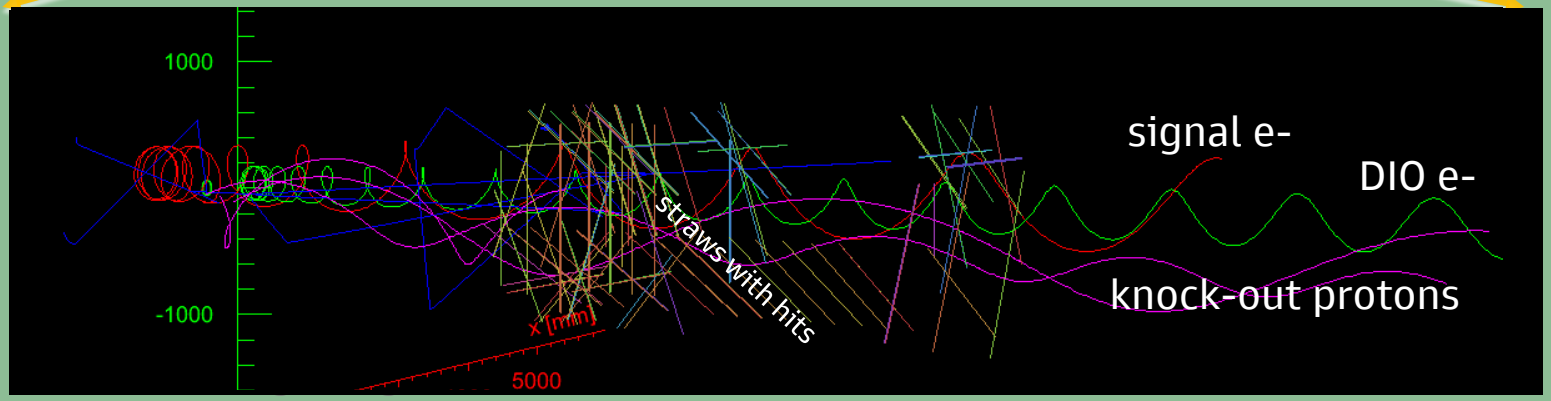

(particles with hits within +/-40 ns of signal electron t_{mean})

- Simulations encompass a full ~1μs, including all the background overlays from the beam flash, μ capture products, neutrons, *etc*. and properly account for contributions from previous bunches.

Mu2e components

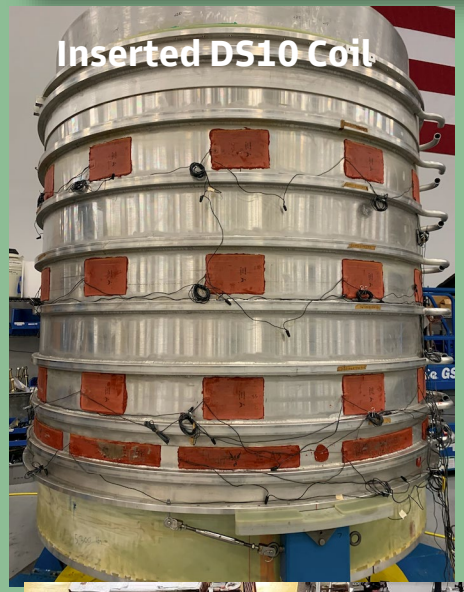

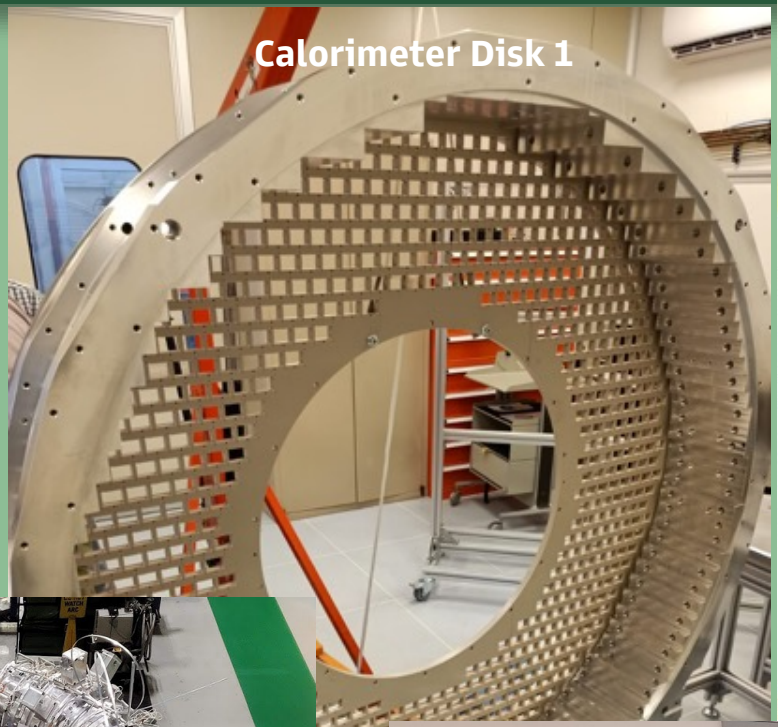

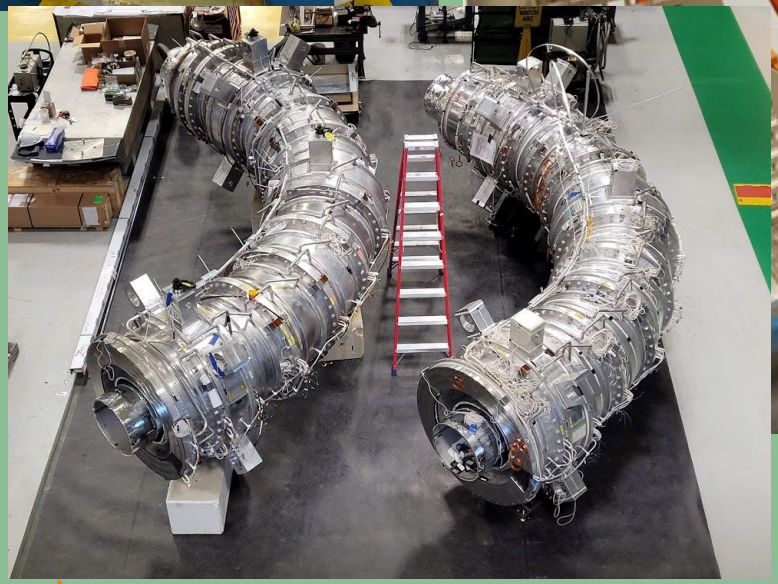

Mu2e schedule/sensitivity

- Beam on target late 2024
- Run 1: 2025-2026 half beam intensity
  - x1000 improvement over SINDRUM-II

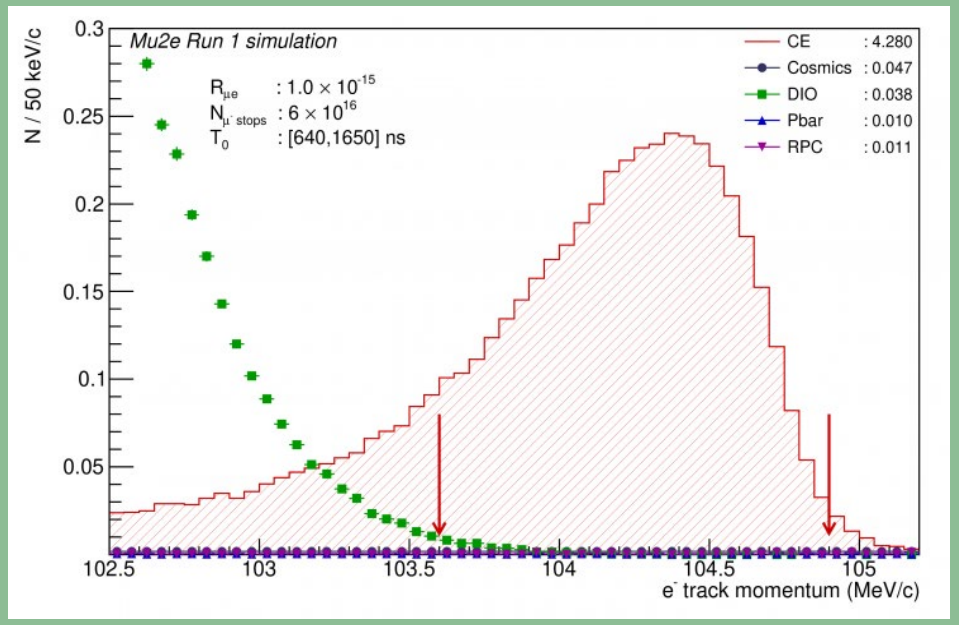

Total background (Cosmics+DIO+RPC+$\bar{p}$) = 0.11±0.03 events

5σ discovery reach

$$R_{\mu e} = 1.1 \cdot 10^{-15}$$

If no events are observed: 90% CL limit:

$$R_{\mu e} = 5.9 \cdot 10^{-16}$$

- Shutdown for PIP-II/LBNF at end of 2026
- Data-taking resumes early 2029 at full beam intensity
  - x10000 improvement over SINDRUM-II 90% CL limit

COMET Phase I

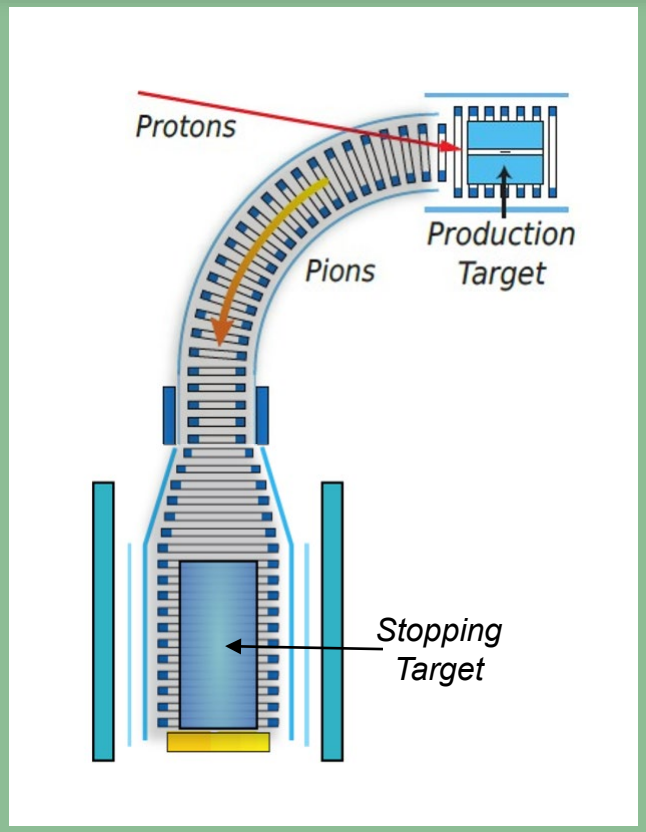

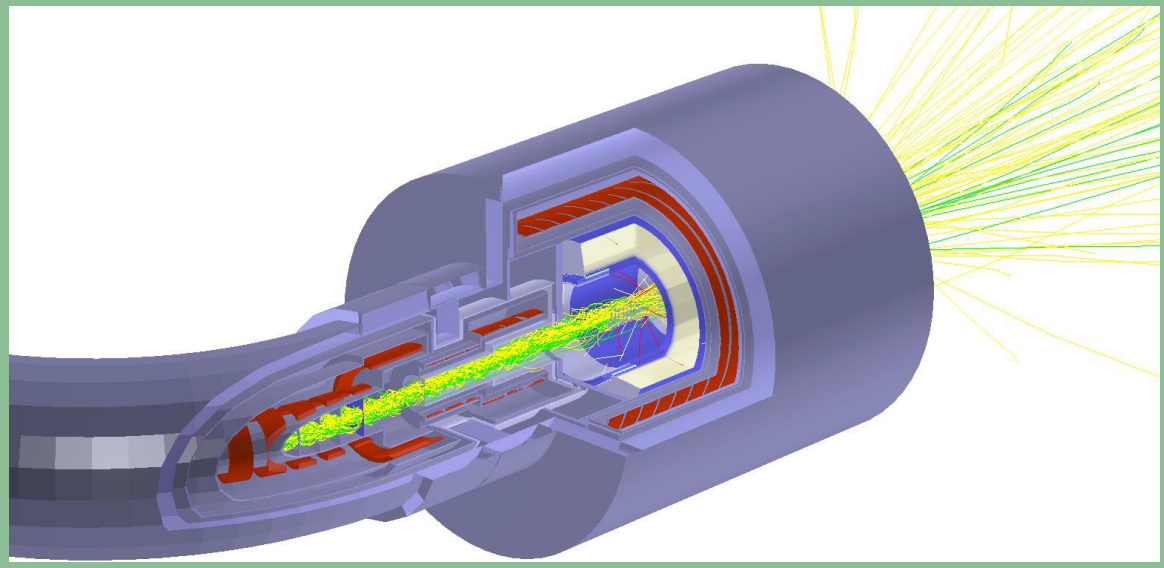

SES 3×10^{-15}
or $< 6 \times 10^{-15}$ @ 90% CL
for 150 days at 3.2 kW

COMET Phase-II

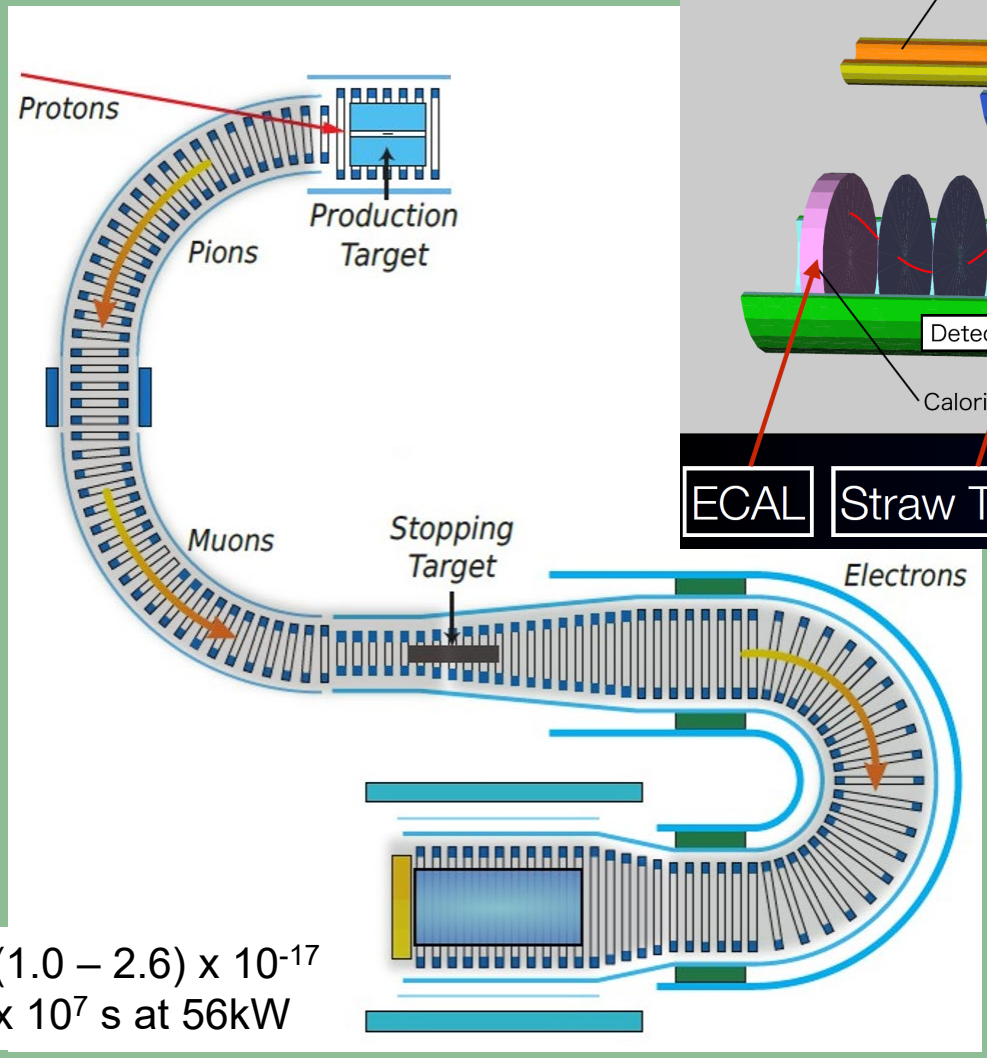

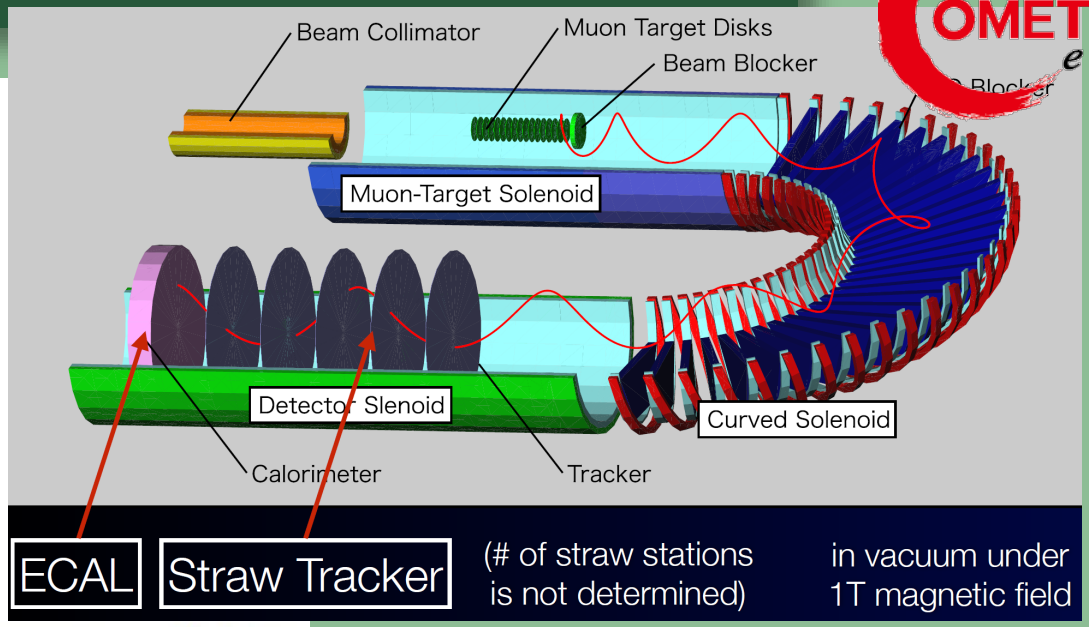

SES (1.0 – 2.6) x 10^{-17}
for 2 x 10^{7} s at 56kW

COMET Phase-I: CyDET(CDC+CTH)

Cylindrical Drift Chamber, constructed in 2016

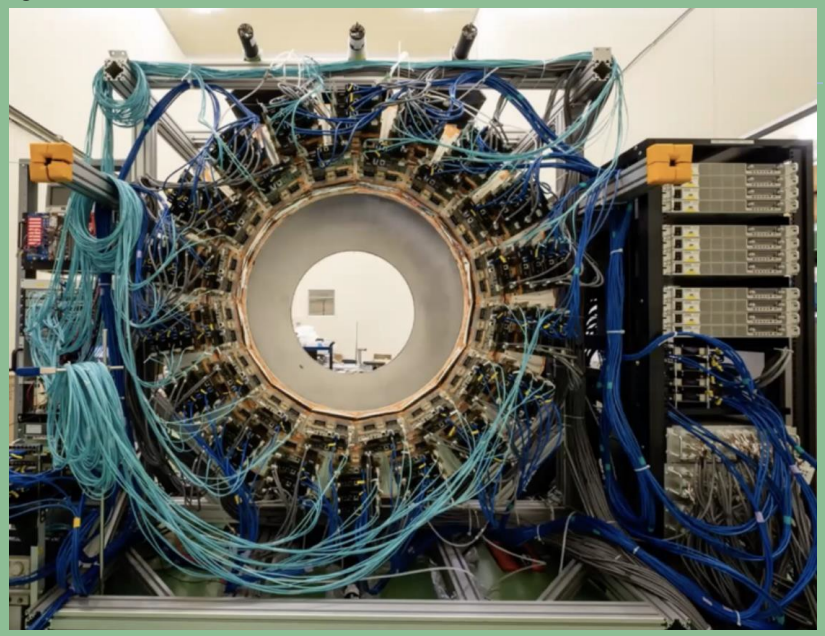

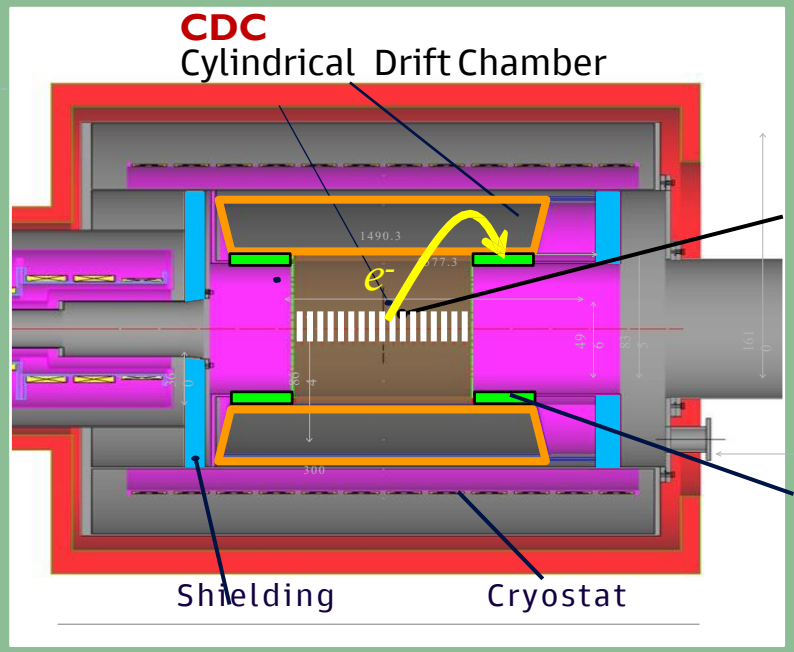

CDC All stereo-wire drift chamber
20 layers, ~5000 sense wires
He:iC_4H_{10} = 9:1 HV=1850V
Momentum resolution
<200keV/c @ 105 MeV/c,
Spatial resolution 170 μm
Cosmic test underway in KEK

CTH 64-segmented two-layered scintillators, providing trigger
~0.8 ns timing resolution

COMET Phase-II

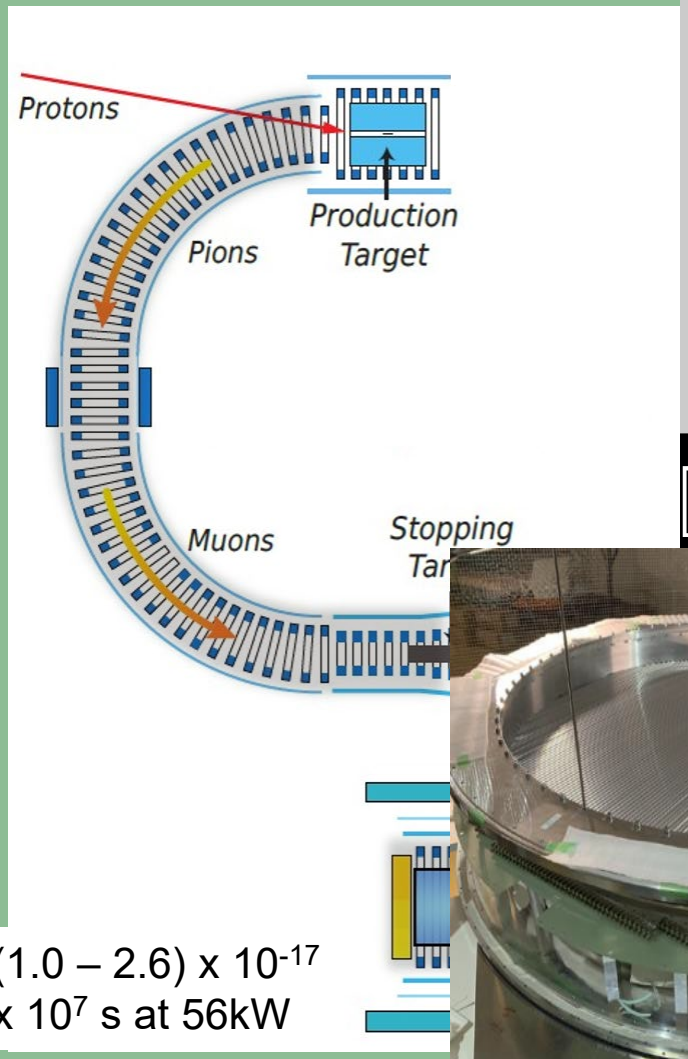

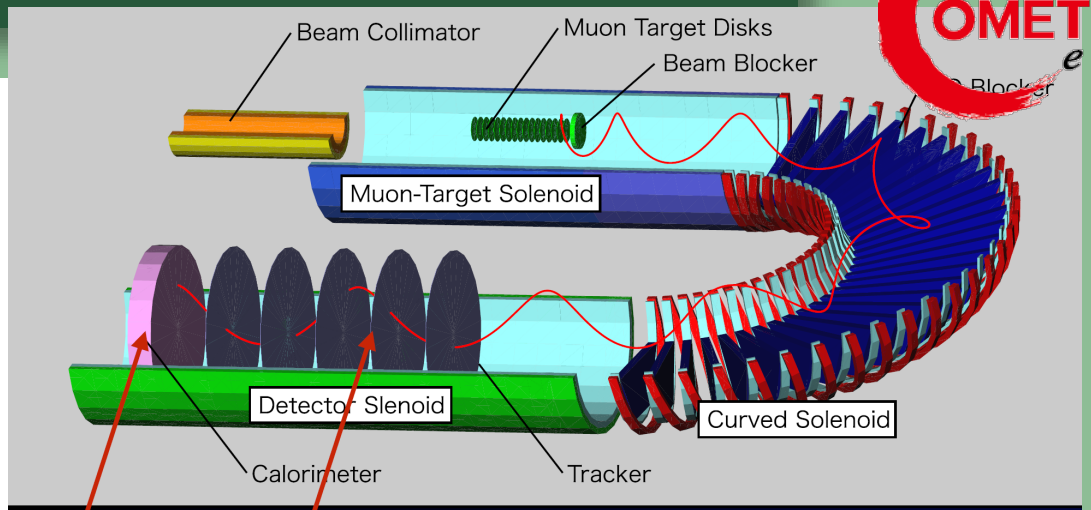

ECAL | Straw Tracker | (# of straw stations is not determined) | in vacuum under 1T magnetic field

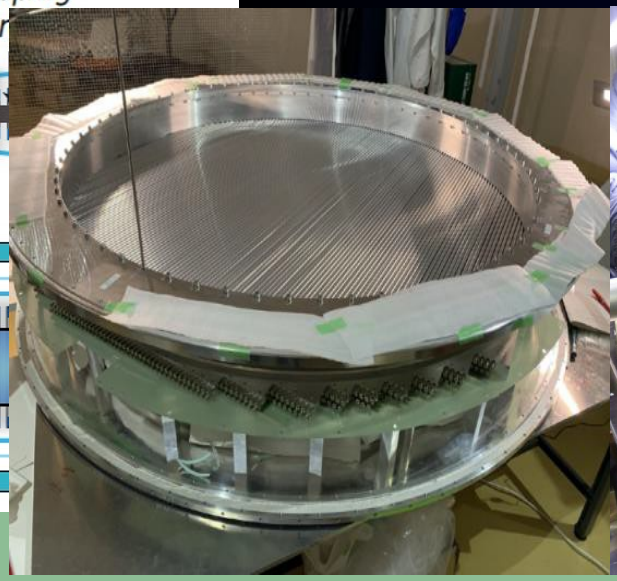

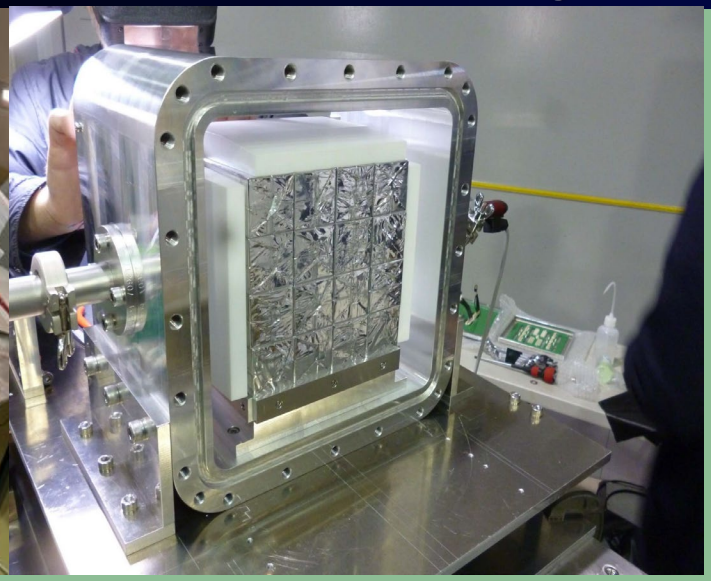

SES (1.0 – 2.6) x 10^{-17}
for 2 x 10^{7} s at 56kW

COMET Phase-I & Phase-II

	COMET-Phase-I	COMET-Phase-II
Experiment starts (*) * including engineering run	in ~2023	Ready in 3 years after completion of Phase-I
Beam power	3.2kW (8GeV, 400nA)	56kW (8GeV, 7μA)
Running time	150 days	2.0×10^{7} (sec)
# of protons	3.0×10^{19}	8.5×10^{20}
# of muon stops	1.5×10^{16}	2.0×10^{18}
Muon rate	5.8×10^{9}	1.0×10^{11}
# of μ stops / p	0.00052	0.00052
Background events	0.02	0.3
S.E.S.	3.1×10^{-15}	2.6×10^{-17}
U.L. (90%CL.)	7.0×10^{-15}	6.0×10^{-17}

Z dependence of μ to e conversion

- If $\mu \to e$ conversion is observed with ^{27}Al, comparison of the conversion rates on different nuclei can provide information on the Lorentz structure of the New Physics

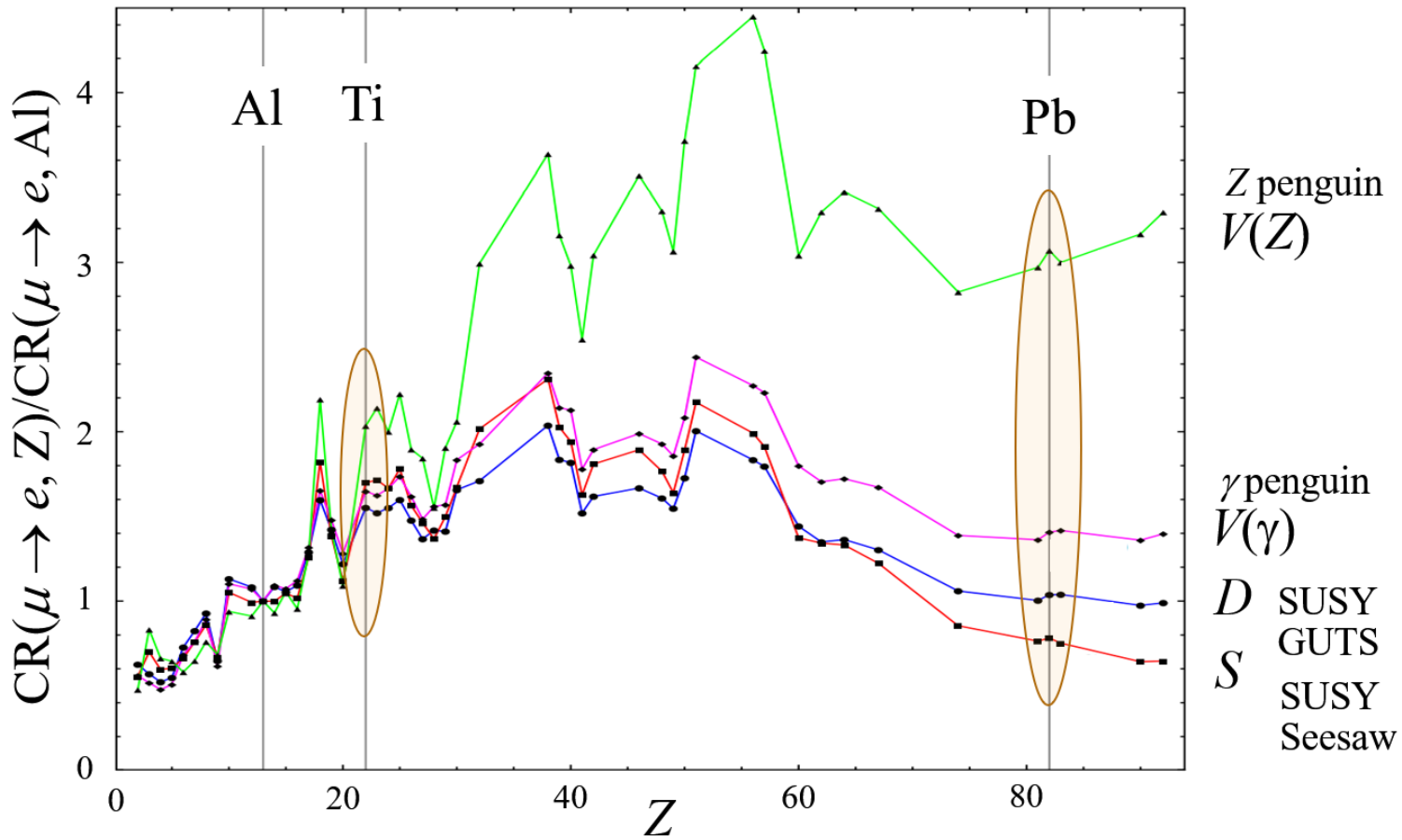

Cirigliano, Kitano. Okada,Tuzon ,*Phys.Rev.D* 80, 013002, 2009

Choice of target

- The choice of a follow-on high Z target involves several considerations
  - Shorter muon lifetime limits the sensitive window

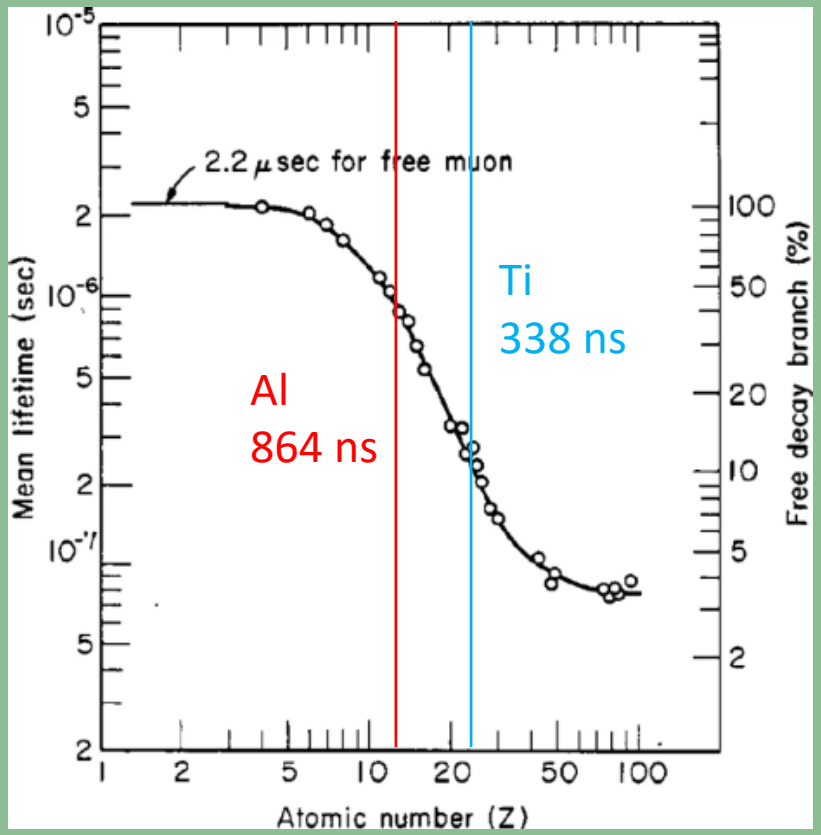

Choice of target

- The choice of a follow-on high Z target involves several considerations
  - Shorter muon lifetime limits the sensitive window
  - Can target be a single isotope or natural abundance?
  - Nuclear spin of target matters
    - As with DM, there are spin-dependent and spin-independent couplings
    - In EFT, each nucleus probes a particular combination of operators, *e.g.* $\tilde{C}^V_{epp}, \tilde{C}^S_{epp}, \tilde{C}^V_{enn}, \tilde{C}^S_{enn}$

Target	Isotopes [abundance]	J	S_p^A, S_n^A	$S_l(m_\mu)/S_l(0)$	B_Z	BR (90% C.L.)
Aluminium	$Z=13$, $A=27$ [100%]	5/2	0.34, 0.030 [21,22]	0.29 [21,22]	132	$\rightarrow 10^{-16}$
Sulfur	$Z=16$, $A=32$ [95%]	0				$< 7\times10^{-11}$ [23]
Titanium	$Z=22$, $A=48$ [74%]	0			234	$< 4.3\times10^{-12}$ [17]
	$Z=22$, $A=47$ [7.5%]	5/2	0.0, 0.21 [24]	~0.12		
	$Z=22$, $A=49$ [5.4%]	7/2	0.0, 0.29 [24]	~0.12		
Vanadium	$Z=23$, $A=50$ [0.25%]	6				
	$Z=23$, $A=51$ [99.75%]	7/2				
Copper	$Z=29$, $A=63$ [70%]	3/2				$BR \leq 1.6\times10^{-8}$ [25]
	$Z=29$, $A=65$ [31%]	3/2				
Gold	$Z=79$, $A=197$ [100%]	5/2	$-(0.52\rightarrow0.30)$, 0.0		285	$BR < 7\times10^{-13}$ [17]
Lead	$Z=82$, $A=206$ [24%]	0				$BR < 4.6\times10^{-11}$ [17]
	$Z=82$, $A=207$ [22%]	1/2	0.0, −0.15 [24]	0.55 [28], ~.026		
	$Z=82$, $A=208$ [52%]	0				

Next steps: PIP2/Mu2e II and HIMB

- PIP2 is a new 800 MeV, 120 kW superconducting linac for LBNF and the muon campus
- There is an active Snowmass study of an upgrade of Mu2e to Mu2e-II
  - An order of magnitude increase in μ^- stops and therefore SES, with only a x3-5 increase in instantaneous rate
  - Detector systems must be upgraded accordingly

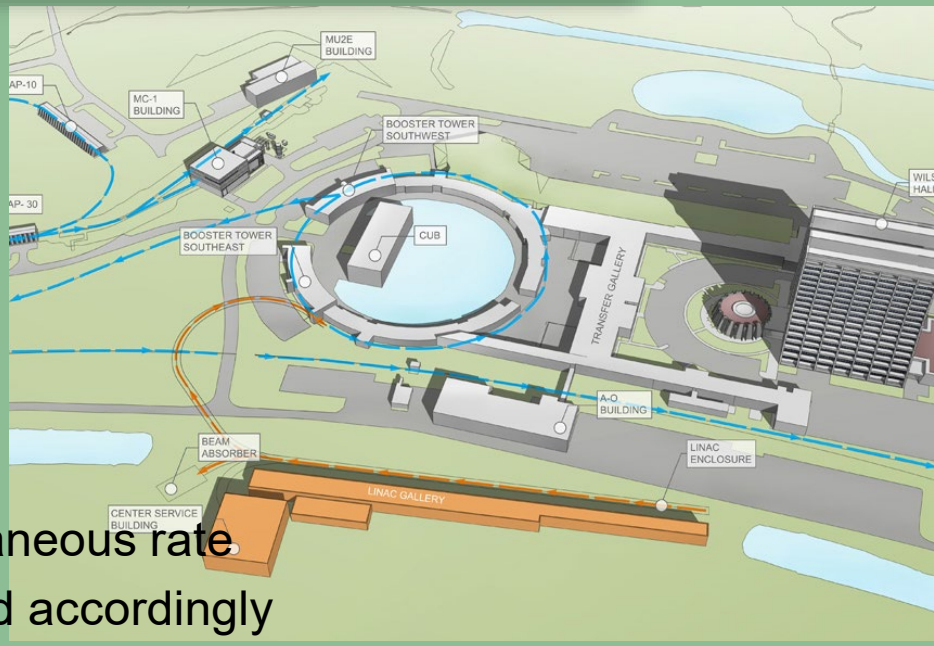

- A surface beam intensity (μ^+) upgrade (HIMB) is being considered at PSI

- "When you come to a fork in the road, take it" – Yogi Berra
  - If $\mu \to e$ conversion has been found, use heavier targets to ascertain the (A, Z) - dependence of conversion rate
  - If $\mu \to e$ conversion is not seen, improve sensitivity of the search

Going further at JPARC and/or Fermilab

Phase Rotated Intense Slow Muon source
PRISM Muon Electron conversion

- A muon storage ring, feeding a COMET-like channel and detector
- High muon intensity: (10^{11}-10^{12} μ^-/s)
- Large 6D acceptance (FFAG)
- Pulsed beam >100 Hz,
- Low momentum, quasi-mono-energetic muons
- Pion contamination <10^{-18}
- Requires a high intensity proton driver
- Aims for SES - 3×10^{-19}
- Time scale well beyond 2030

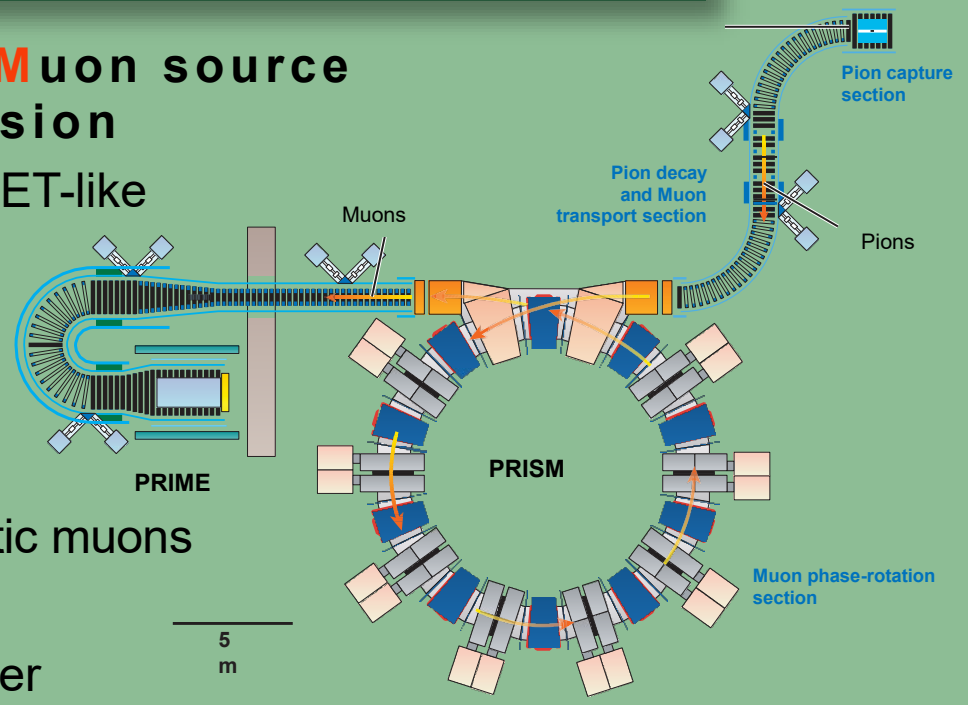

- A similar concept with protons from PIP2 is now taking shape at Fermilab as part of the Snowmass exercise
  - Aims at μ^+ and μ^- beams to cover a full spectrum of CLFV experiments

Outlook

- Current limits on charged lepton flavor violation provide useful constraints on many New Physics models
- Over the next decade, improved μ decay, leptonic and semileptonic meson decay, $\mu \to e$ conversion and τ decay experiments will have the sensitivity to probe the regime predicted by many New Physics models
  - Sensitivities reach well beyond what is possible in direct production of new particles at the LHC
  - Should evidence for CLFV be found, comparison of branching ratios and conversion rates will be diagnostic of specific models